

Monte Carlo Approach for Transmission Probability & Radiation Heat Load and CFD Analysis for Cryopump Application

By

Rana Chirag Rameshbhai

(10MMCC13)



DEPARTMENT OF MECHANICAL ENGINEERING

INSTITUTE OF TECHNOLOGY

NIRMA UNIVERSITY

AHMEDABAD-382481

MAY 2012

Monte Carlo Approach for Transmission Probability & Radiation Heat Load and CFD Analysis for Cryopump Application

Major Project

Submitted in Partial Fulfillment of the Requirements

for the degree of

**Master of Technology in Mechanical Engineering
(CAD/CAM)**

Prepared By

Rana Chirag Rameshbhai

(10MMCC13)

Guided by

Prof.V.R.Iyer

Mr.Raviprakash.N



DEPARTMENT OF MECHANICAL ENGINEERING

INSTITUTE OF TECHNOLOGY

NIRMA UNIVERSITY

AHMEDABAD-382481

MAY 2012

Declaration

This is to certify that

- i) The thesis comprises my original work towards the degree of Master of Technology in Mechanical Engineering(CAD/CAM) at Nirma University and has not been submitted elsewhere for a degree.
- ii) Due acknowledgement has been made in the text to all other material used.

Rana Chirag Rameshbhai
(10MMCC13)

Undertaking for Originality of the Work

I, **Rana Chirag Rameshbhai**, Roll. No.10MMCC13 , give undertaking that the Major Project entitled “**Monte Carlo Approach for Transmission Probability & Radiation Heat Load and CFD Analysis for Cryopump Application**” submitted by me, towards the partial fulfillment of the requirements for the degree of Master of Technology in **Mechanical Engineering(CAD/CAM)** of Nirma University, Ahmedabad, is the original work carried out by me and I give assurance that no attempt of plagiarism has been made. I understand that in the event of any similarity found subsequently with any published work or any dissertation work elsewhere; it will result in severe disciplinary action.

Signature of Student

Date:_____

Place: NU, Ahmedabad

Endorsed by

(Signature of Guide)

Certificate

This is to certify that the Major Project Report entitled “**Monte Carlo Approach for Transmission Probability & Radiation Heat Load and CFD Analysis for Cryopump Application**” submitted by **Mr. Rana Chirag Rameshbhai (10MMCC13)**, towards the fulfillment of the requirements for **Master of Technology in Mechanical Engineering(CAD/CAM)** of Nirma University is the record of work carried out by his under our supervision and guidance. The work submitted has reached a level required for being accepted for examination. The results embodied in this major project, to the best of our knowledge have not been submitted to any other University or Institution for award of any degree or diploma.

Date:

Industrial Guide

Raviprakash N.

Engineer SF

Head, RHRTD

Institute For Plasma Research

Gandhinagar

Institute Guide

Prof.V.R.Iyer

Principal

Institute of Diploma Studies

Nirma University

Ahmedabad

Head of Department

Dr.R.N Patel

Department of Mechanical Engineering

Institute of Technology

Nirma University

Ahmedabad

Director

Dr.K.Kotecha

Institute of Technology

Nirma University

Ahmedabad

Acknowledgements

With immense pleasure, I would like to present this report on the part of my dissertation work related to “Monte Carlo Approach for Transmission Probability & Radiation Heat Load and CFD Analysis for Cryopump Application”. I am very thankful to all those who helped me for the successful completion of the dissertation and for providing valuable guidance throughout the project work.

This work is carried out and financially supported by, NFP-Program, Institute For Plasma Research, Gandhinagar.

I hereby take the opportunities to express my deep sense of gratitude to my respected industry guides, **Mr. Raviprakash.N.** I heartily thank them for their time to time suggestion and the clarity of the concepts of the topic that helped me a lot during the study.

I would like to thank **Ms. Ranjana Gangradey**, Scientist ‘SE’, Mr. Pratik Nayak, Scientific Assistant ‘B’, Mr. Navnath Mandlik (Senior Engineer, Tata consultancy Engineering, Mumbai) for providing me valuable suggestion to carry out my project.

I would like to offer thanks to **Prof. V.R. Iyer**, Institute Guide who helped me in pointing the need of the project, suggestions and encouragement during the time of research and also for writing of this report.

My sincere thanks and gratitude to **Dr. D.S. Sharma**, PG-Coordinator, CAD/CAM, **Dr. R.N. Patel**, Head, Mechanical Engineering Department, Institute of Technology, Nirma University, Ahmedabad for their continual kind words of encouragement and motivation throughout the Dissertation work.

Finally, I would like to thank The Almighty, my family members for supporting and encouraging me in all possible ways. I would also like to thank my friends who have provided continuous encouragement in making this dissertation work successful.

Rana Chirag Rameshbhai
(10MMCC13)

Abstract

In fusion Reactor during fusion process exhaust gases are produced. The gases produced contain mainly isotopes of hydrogen and helium. So exhaust gases must remove from the fusion reactor. Removal of exhaust gases required very high pumping system. For fusion reactor Vacuum pumping system is facing challenges. The operation of mechanical pump with rotating parts faces problems due to eddy currents. Cryopump which has all static parts is an option to pump such machines. For this requirement cryopump is used. Cryopump is mainly designed for maximum transmission probability, minimum radiation heat load on cryopanel and optimum temperature of gas particle striking on cryopanel. Geometry has to be optimized for it. Flow distribution of liquid He in cryopanel for liquid helium flow through cryopanel should be uniform and it maintains cryopanel temperature for cryopumping.

Molecular flow can be simulated by Movak 3D software. In Movak 3D, modeling of geometry for simulation is difficult task due to repeat command logic development for new geometry. For that, use of CAD tool generation of complicated geometry is possible for it. Most of work is generation for modeling geometry for it with use of basic command like triangle, parallelogram, circle, ring, cone. Thus, using with 3D transformation command (CAD feature) complicated geometry can be generated efficiently. And transmission probability of cryopump is geometry dependent. By varying geometry feature, geometry is optimized for this situation. Movak 3D code allows Monte Carlo Ray Tracing method for radiation analysis. In development of single panel cryopump Radiation heat load approximation is necessary. So by using Movak 3D code, radiation heat load on main component of single panel cryopump was find out and CFD analysis was done in Ansys Fluent for flow distribution in cryopanel channel.

Abbreviations

IPR	Institute For Plasma Research
TPMC	Test Particle Monte Carlo Simulation
DSMC	Direct Simulation of Monte Carlo
TP	Transmission Probability
CFD	Computational Fluid Dynamics
VF	View Factor
JET	Joint Europe Tourse
MFTF	Mirror Fusion Test Facility
UHV	Ultra High Vacuum
LHCD	Lower Hybrid Current Drive
FZK	Karlsruhe Research Center
LN	Liquid Nitrogen
ITER	International Thermonuclear Experimental Reactor
LHe	Liquid Helium
ScHe	Super Critical Helium

Contents

Declaration	iii
Undertaking for Originality of the Work	iv
Certificate	v
Acknowledgements	vi
Abstract	vii
Abbreviations	viii
List of Figures	xii
List of Tables	3
1 Introduction	4
1.1 Basics of Plasma	4
1.2 Introduction to Fusion Power	5
1.3 How Fusion Works	6
1.4 Institute For Plasma Research	7
1.5 ITER	8
1.6 Fusion Reactor Cryopump	10
1.7 Cryopump	11
2 Project Details and Methodology	12
2.1 Project Title	12
2.2 Description of Project Work	12
2.2.1 Molecular Flow Analysis	12
2.2.2 Radiation Analysis	13
2.2.3 Fluid Analysis	13
2.3 Methodology	13

3	Literature Survey	16
3.1	Molecular Flow Analysis	16
3.1.1	Cryopump	16
3.1.2	Cryopump Design	16
3.1.3	Thermal Accommodation	18
3.1.4	Transmission Probability	19
3.1.5	Various Approach for Pumping Speed	19
3.1.6	Monte Carlo Simulation	19
3.1.7	Monte Carlo Simulation for Chevron Baffle Performance	20
3.2	Radiation Analysis	21
3.2.1	Radiation	21
3.2.2	Gray Body Radiation Heat Transfer	22
3.3	Fluid Analysis for Cryopanel	24
4	CAD Work in Geometric Modeling in Movak 3D	25
4.1	Movak 3D Programming	25
4.2	Programming Step and its Meaning for Main Component of Cryopump	26
5	Molecular Flow Analysis	31
5.1	Movak 3D	32
5.1.1	Geometric Modeling of the Apparatus	32
5.1.2	A Surface Property Assignment	32
5.1.3	Running a Monte-Carlo Simulation	33
5.1.4	Geometric Modeling Base	33
5.2	Experimental Verification for Movak 3D Transmission Probabiliy Result	35
5.2.1	Verification of Transmission Probability for Pipe Geometry with Literature and Movak3D Simulation	35
5.2.2	Transmission Probability Experimental Bench Marking (Titan Test Facility)	39
5.3	Project Work Done	43
5.3.1	Back Ground of Work	43
5.3.2	Industrial Cryopump	44
5.3.3	Helix Geometry	47
5.3.4	Multi Panel Cryopump	50
5.3.5	Tubing Multipanel Cryopump	54
5.3.6	Pumping Speed Calculation	58
6	Radiation Analysis	60
6.1	Radiation	60
6.1.1	Gray Body Radiation Heat Transfer	60
6.1.2	Theory for Monte Carlo Ray Trace Method	61
6.2	Radiation Bench Marking	62
6.2.1	Problem 1	62

6.2.2	Verification of Radiation Heat Load by Various Approach for Cylinder Case	66
6.2.3	Radiation Analysis Bench Mark with Ansys	71
6.3	Project part :- Radiation Heat Load Analysis For Single Panel Cryopump by Movak 3D	73
6.4	Radiation Heat Load Minimization in Single Panel Cryopump	77
6.4.1	Minimization of Radiation Heat Load on Cryopanel	77
6.4.2	Result of Movak 3D Simulation for Modified Emissivity	77
7	CFD Analysis For Cryopanel	79
7.1	Cryopanel Fluid Analysis	79
7.2	Cryopanel Thermal Fluid Analysis	79
7.3	Bench marking	80
7.3.1	Pressure Drop in Circular Pipe	80
7.3.2	Simulation of Pressure Drop in Ansys Fluent	81
7.3.3	Nozzle Velocity	83
7.3.4	Analysis of Nozzle	84
7.4	Project Part Analysis	86
7.4.1	Seam Welded cryopanel	86
7.4.2	Bubble Form Cryopanel	89
8	Results	93
8.1	Molecular Flow Analysis	93
8.2	Radiation Analysis	93
8.3	CFD Analysis	94
9	Conclusion and Future Scope	95
9.1	Future Scope	96
A	Property	97
	References	98

List of Figures

1.1	Plasma: The Fourth State Of Matter	5
1.2	Plasma: The Fusion Reaction	6
1.3	Achieving Fusion Power	7
1.4	ITER Machine	9
1.5	Schematic Diagram of Cryopump	11
2.1	Project Detail Chart	15
3.1	Chevron Baffle	20
3.2	Result For The Three Baffle Configurations as a Function of Baffle Angle α . Solid Line, Chevron Configuration, Short Dashed Line, Offset Configuration; Long Dashed Line, Offset Configuration With β fixed At 90° , +Measured, *Calculated For Chevron Baffle	20
4.1	Program for Defining Variable, Title, Absolute Point, Relative Point, Surfaces, Surface Property for Outer Surface.	26
4.2	Programming Step for 24 Cryopanel Generation. It Include 3D Transformation Mathematical Logic and set in Programm Line Command.	27
4.3	Movak 3D Generated Model of 24 Cryopanel (result of Program Logic).	28
4.4	Defining 15 Baffle of Cryopump, Which is Created by Using Repeat Loop and Increment of Distance in The Code.	29
4.5	Final CAD Model Done In Cryopump due to Programming of Dome, Cryopanels and Louver Baffles.	30
5.1	Pipe Model in Movak 3D	36
5.2	Particle Simulation in Pipe	38
5.3	Titan Test Facility: Cross-Section and Monte Carlo Model	39
5.4	Titan Test Facility Modeling In Movak 3D In Research Paper	41
5.5	Titan Test Facility Modeling in Movak 3D for Validation	41
5.6	Titan Test Facility Modeling Particle Trajecory for 50 Particle	42
5.7	Industrial Cryopump Movak 3D Modeling	45
5.8	Transmision Probabiliy Result for Indusrial Crryopump	46
5.9	Helix Modeling in Movak 3D	48

5.10	Chart For 80 ^o K and TP Optimization	49
5.11	Multipanel Cryopump Movak 3D Modeling	51
5.12	3D View of Multipanel Design	52
5.13	Multipanel Cryopump Modification 1 Movak 3D Modeling	52
5.14	Multipanel Cryopump Modification 2 Movak 3D Modeling	53
5.15	Initial Tubing Multipanel Cryopump Movak 3D Modeling	55
5.16	3D View Tubing Multipanel Cryopump Movak 3D Modeling	56
5.17	Tubing Multipanel Cryopump Modification 1 Movak 3D Modeling	56
5.18	Tubing Multipanel Cryopump Modification 2 Movak 3D Modeling	57
5.19	Templet for Various Geometry	59
6.1	Iter Preproduction Cryopump Bench Marking Problem of Paper Monte Carlo Model	62
6.2	Simulation Model in Movak 3D	63
6.3	Simulation Result for Case 1	64
6.4	Simulation Result for Case 2	64
6.5	Comparison of Movak 3D View Factor Result with Paper Result	65
6.6	Bench Mark Case Model	66
6.7	Heat Load Bench Mark Case 2	68
6.8	MOVAK 3D HEAT LOAD	70
6.9	Geometry for Ansys Bench Marking	71
6.10	Movak 3D Result for Ansys Bench Marking	72
6.11	Movak 3D Model for Single Panel Cryopump	75
6.12	Movak 3D Result for Single Panel Cryopump	75
6.13	Movak 3D Heat Load Distribution for Single Panel Cryopump	76
6.14	Movak 3D Heat Load Distribution for Optimized Emissivity Single Panel Cryopump	77
7.1	Modeling of Pipe	81
7.2	Meshing of Pipe	82
7.3	Pressure Drop in Pipe	82
7.4	Meshing of Nozzle	84
7.5	Pressure Drop in Nozzle	84
7.6	Velocity in Nozzle	85
7.7	Seam Welded Cryopanel Dimension	86
7.8	Seam Welded Cryopanel	87
7.9	Meshing of Seam Welded Cryopanel	87
7.10	Temperature Profile of Seam Welded Cryopanel	88
7.11	Pressure Profile of Seam Welded Cryopanel	88
7.12	Bubble Cryopanel Dimension	89
7.13	Bubble Cryopanel Dimension	90
7.14	Meshing of Bubble Cryopanel	90
7.15	Pressure Profile of Bubble Cryopanel	91

7.16 Temperature Profile of Bubble Cryopanel	91
7.17 Velocity vector Profile of Bubble Cryopanel	92

List of Tables

3.1	Comparison Of Initial (Zero Gas Load) Sticking Probability for Nuclear Fusion Relevant Gases at Different Temperature	17
5.1	Comparison with Movak 3D Simulation Result with Theorititcal Correction Factor Result	38
5.2	Titan Test Experimental Validation Compare With Movak 3D Code Result	42
5.3	Movak3D boundary condition for industrial cryopump	44
5.4	Movak 3D surface utilization for indutrial cryopump CAD modeling	44
5.5	Thermal Boundary Condiation for Temp and Thermal Accomodation for Helix	47
5.6	Movak 3D modeling surface utilization for helix.	47
5.7	Helix Reult for 80-90°K Particle and Transmission Probability(*where parti=particle)	49
5.8	Movak 3D Thermal Boundary Condition for Multipanel Cryopump .	50
5.9	Movak 3D Surface Utilization for Multipanel Cryopump	50
5.10	Movak 3D Result for Transmission Probability and 80°K-90°K Particle for Multipanel Cryopump	53
5.11	Movak 3D Boundary Condition for Tubing Multipanel Cryopump . .	54
5.12	Movak 3D Surface Utilization for Tubing Multipanel Cryopump . . .	54
5.13	Movak 3D Result For 0.1 Thermal Accomodation and 80°K-90°K Particle	57

5.14	Pumping Speed for Tubing Multipanel Cryopump	58
6.1	Comparison with Movak 3D Heat Load Data with Standard Literature Data in Terms of Watt	65
6.2	Temperature and Emissivity Data for Cylinder Geometry Bench Mark- ing Case	67
6.3	View Factor for Cylinder Surface	67
6.4	Heat Load Distribution on Cylinder Surface	68
6.5	Probable Movak 3D Particle Distribution for MCRT Approach	69
6.6	Particle Distribution in Movak 3D for 10,00,000	69
6.7	Heat Exchanger Factor for Pipe Case	69
6.8	Heat Load Distribution in Terms of Watt By MCRT Approach	70
6.9	Comparison of Various Approach for Heat Load Data	70
6.10	Boundary Condition for Ansys View Factor Case for Radiation Heat Load Study	71
6.11	Boundary Condition for Single Panel Cryopump	74
6.12	Surface Element Include for Single Panel Cryopump	74
6.13	Heat Load Distribution for Single Panel Cryopump	76
7.1	Water Property for 20 C	80
7.2	Water Property	83
7.3	Liquid Helium Property at 4.2K	87
7.4	Property for Liquid Helium at 4.2K	90
A.1	Liquid helium property at lower temperature	97

Chapter 1

Introduction

1.1 Basics of Plasma

Plasma is a partially ionized gas, in which a certain proportion of electrons are free rather than being bound to an atom or molecule. The ability of the positive and negative charges to move somewhat independently makes the plasma electrically conductive so that it responds strongly to electromagnetic fields. Plasma therefore has properties quite unlike those of solids, liquids or gases and is considered to be a distinct state of matter.

Plasma typically takes the form of neutral gas-like clouds, as seen, for example, in the case of stars. Like gas, plasma does not have a definite shape or a definite volume unless enclosed in a container. Plasmas actually make up nearly 99 percent of the matter in the universe but is extremely rare on Earth. Plasmas resulting from ionization of neutral gases generally contain equal numbers of positive and negative charge carriers. Such plasmas are termed quasi-neutral. Strongly non-neutral plasmas, which may even contain charges of only one sign, occur primarily in laboratory experiments: their equilibrium depends on the existence of intense magnetic fields, about which the charged fluid rotates.

The “fourth aggregate state of matter”, largely composed of ionised atoms or

molecules and their free electrons. Fusion-oriented high-temperature plasma physics is concerned with ionised hydrogen.[35]

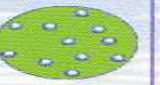
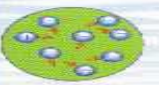
Solid	Liquid	Gas	Plasma
Example Ice H_2O	Example Water H_2O	Example Steam H_2O	Example Ionized Gas $H_2 \rightarrow H^+ + H^+ + 2e^-$
Cold $T < 0^\circ C$	Warm $0 < T < 100^\circ C$	Hot $T > 100^\circ C$	Hotter $T > 100,000^\circ C$ $I > 10$ electron Volts
			
Molecules Fixed in Lattice	Molecules Free to Move	Molecules Free to Move, Large Spacing	Ions and Electrons Move Independently, Large Spacing

Figure 1.1: Plasma: The Fourth State Of Matter

1.2 Introduction to Fusion Power

Nuclear fusion is one of the most promising options for generating large amounts of carbon-free energy in the future. Fusion is the process that heats the Sun and all other stars, where atomic nuclei collide together and release energy (in the form of neutrons). Fusion scientists and engineers are developing the technology to use this process in tomorrow's power stations. To get energy from fusion, gas from a combination of types of hydrogen - deuterium and tritium - is heated to very high temperatures (100 million degrees Celsius). One way to achieve these conditions is a method called 'magnetic confinement' - controlling the hot gas (known as plasma) with strong magnets. The most promising device for this is the 'tokamak', a Russian word for a ring-shaped magnetic chamber.[35]

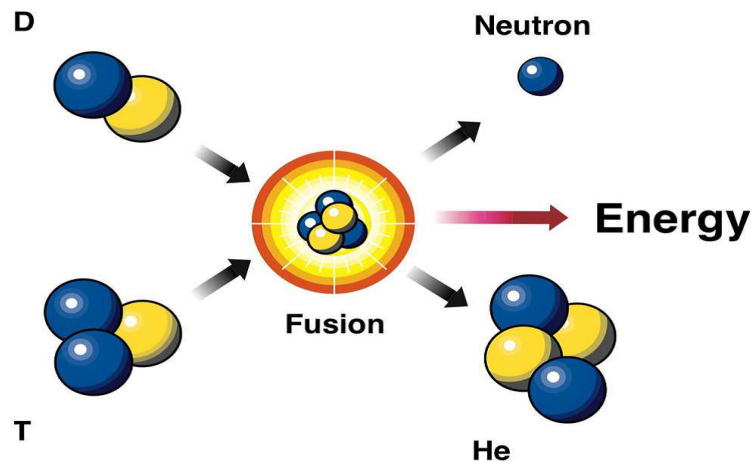


Figure 1.2: Plasma: The Fusion Reaction

1.3 How Fusion Works

The incredibly hot plasma is extremely thin and fragile, a million times less dense than air. To keep the plasma from being contaminated and cooled by contact with material surfaces it is contained in a magnetic confinement system. A plasma of light atomic nuclei is heated and confined in a circular bottle known as a tokamak, where it is controlled with strong magnetic fields. In a magnetic fusion device, the maximum fusion power is achieved using deuterium and tritium. These fuse to produce helium and high-speed neutrons, releasing 17.6MeV (mega electron volts) of energy per reaction. This is approximately 10,000,000 times more energy than is released in a typical chemical reaction. A commercial fusion power station will use the energy carried by the neutrons to generate electricity. The neutrons will be slowed down by a blanket of denser material surrounding the machine, and the heat this provides will be converted into steam to drive turbines and put power on to the grid.[35]

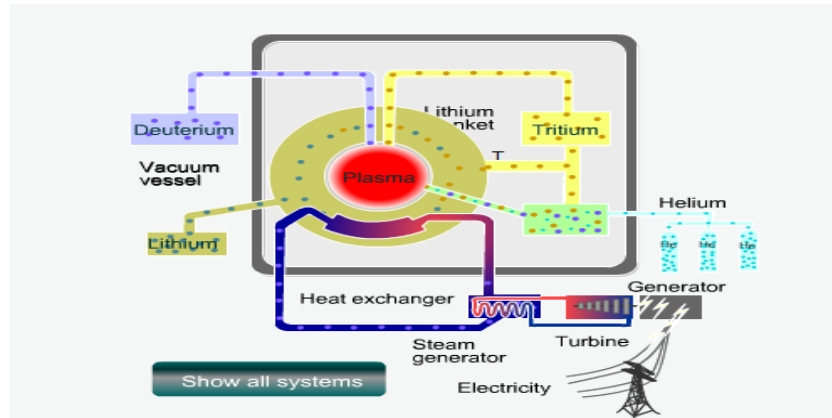


Figure 1.3: Achieving Fusion Power

1.4 Institute For Plasma Research

The Institute for Plasma Research can trace its roots back to early 1970's when a coherent and interactive programme of theoretical and experimental studies in plasma physics with an orientation towards understanding space plasma phenomena was established at the Physical Research laboratory. The early studies were on simulation of $E \times B$ instabilities characteristic of the equatorial electrojet, plasma-neutral gas interaction with relevance to the cometary plasma-solar wind interaction and single particle confinement in non-adiabatic magnetic mirrors. Experiments on non-linear ion acoustic waves and double layers were added later. High power plasma experiments using intense electron beams to form compact toroids and electron rings in toroidal devices started in 1978 reflected a re-orientation to fusion-relevant experiments.

A proposal to the Government of India to initiate studies on magnetically confined high temperature plasmas was accepted in 1982 and resulted in establishment of the Plasma Physics Programme (PPP) supported by the Department of Science and Technology. Design and engineering of India's first tokamak ADITYA started at the same time. In 1984 the activities moved into an independent campus at Bhat village in the outskirts of Ahmedabad city in 1984. The PPP evolved into the autonomous

Institute for Plasma Research under the Department of Science and Technology in 1986. With the commissioning of ADITYA in 1989, full-fledged tokamak experiments started. A dynamic experimental programme focusing on transport due to edge turbulence has resulted in major discoveries in this field. This period also saw development of new programmes in plasma processing and basic and computational plasma research.

With the decision to build the second generation superconducting steady state tokamak SST-1 capable of 1000 second operation in 1995, the institute grew rapidly and came under the administrative umbrella of the Department of Atomic Energy. Major new programmes in pulsed power, advanced diagnostics, computer modelling, development of RF and neutral beam heating systems etc. also came into being. The industrial plasma activities were reorganised under the Facilitation Centre for Industrial Plasma Technologies and moved to a separate campus in Gandhinagar in 1998.

IPR is now internationally recognized for its contributions to fundamental and applied research in plasma physics and associated technologies. It has a scientific and engineering manpower of 200 with core competency in theoretical plasma physics, computer modeling, superconducting magnets and cryogenics, ultra high vacuum, pulsed power, microwave and RF, computer-based control and data acquisition and industrial, environmental and strategic plasma applications.[34]

1.5 ITER

ITER is an international Tokamak research/engineering project designed to prove the scientific and technological feasibility of a full-scale fusion power reactor. It is an experimental step between today's studies of plasma physics and future electricity-producing fusion power plants. The heart of ITER is a superconducting Tokamak facility with striking design similarities to JET, but twice the linear dimensions. It will have a plasma volume of around $840m^3$. It is designed to produce approximately

500 MW of fusion power sustained for more than 400 seconds. ITER will be the first fusion experiment with an output power higher than the input power.

On November 21st 2006, the seven participants (European Union, India, Japan, Korea, People's Republic of China, Russian Federation and United States of America) formally agreed to fund the project. The ITER programme is anticipated to last for 30 years - 10 years for construction, and 20 years of operation. It will be based in Cadarache, France. It is technically ready to start construction and the first plasma operation is expected in 2016. The main parts of the ITER tokamak reactor are:

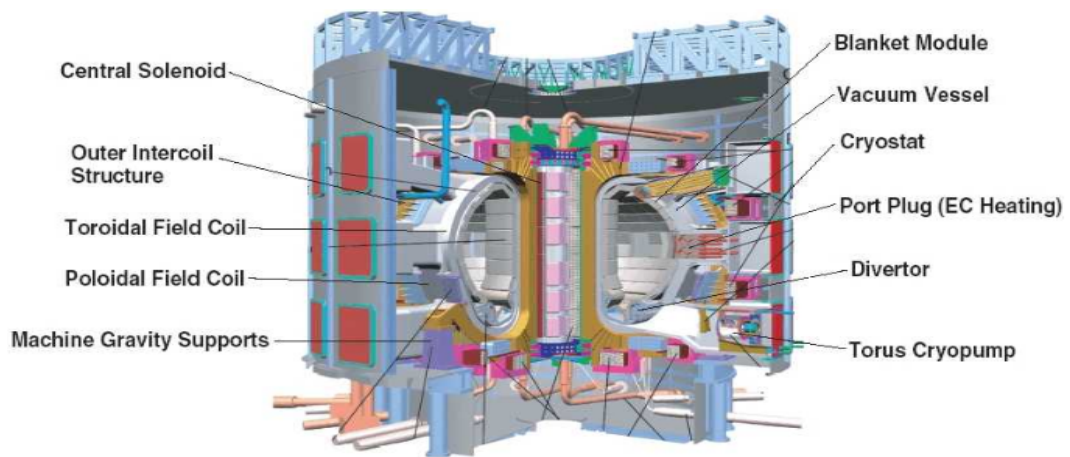


Figure 1.4: ITER Machine

- Vacuum vessel - holds the plasma and keeps the reaction chamber in a vacuum.
- Neutral beam injector (ion cyclotron system) - injects particle beams from the accelerator into the plasma to help heat the plasma to critical temperature.
- Magnetic field coils (poloidal, toroidal) - super-conducting magnets that confine, shape and contain the plasma using magnetic fields.
- Transformers/Central solenoid - supply electricity to the magnetic field coils.
- Cooling equipment (cryostat, cryopump) - cool the magnets.

- Blanket modules - made of lithium; absorb heat and high-energy neutrons from the fusion reaction.
- Divertors - exhaust the helium products of the fusion reaction.[33]

1.6 Fusion Reactor Cryopump

Control of the gas throughput, especially the helium ash produced by D-T fusion reactions, is one of the key issues affecting the performance and achievable burn time of a fusion reactor.

The ITER machine includes three large cryogenic high-vacuum pumping systems. One is for Evacuation and maintenance of the required pressure levels in the torus (1350 m^3), the second is for generation of the required vacuum conditions in the neutral beam injectors (NBI) (570 m^3), which are used to heat up the plasma by injection of highly energetic accelerated neutral H and D particles, and the third is for provision of the insulation vacuum in the cryostat (8400 m^3), which houses the super conducting coil system. The typical pressures inside the torus and the NBI systems are in the range of 1 to 10 Pa.

As fusion reactor will be a burning deuterium-tritium plasma experiment, the vacuum system must not only be designed for the high magnetic and electric fields but also withstand disruption events creating high mechanical loads, radiation, and be compatible with tritium. The latter excludes the use of any organic material in direct or sealing contact with the process gas. These requirements can be met best with cryogenic pumps without any moving parts. All large high-vacuum pumping systems on ITER are based on charcoal-coated cryopanel forced-cooled by $4.5\text{ }^\circ\text{K}$ supercritical helium at 0.4 MPa. The Cryopumping is a demanding field because it cross-links many different disciplines such as vacuum science, cryogenic engineering, surface and physical chemistry. It further brings together in a unique way technological and physics aspects. In view of the large Research and development coming up in the next few years.[1][6]

1.7 Cryopump

A cryopump is defined as a vacuum pump which captures the gas by surfaces cooled to temperatures below 120 °K.

Cryopumps are commonly cooled by compressed helium though they may also use dry ice, liquid nitrogen, or stand-alone versions may include a built-in cryocooler. Baffles are often attached to the cold head to expand the surface area available for condensation, A cryopump is a vacuum pump that traps gases and vapors by con-

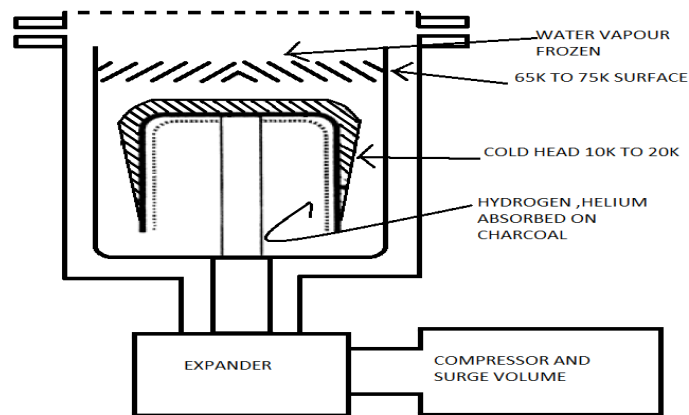


Figure 1.5: Schematic Diagram of Cryopump

densing them on a cold surface. They are only effective on some gases, depending on the freezing and boiling points of the gas relative to the cryopump's temperature. Cryopumps are often combined with sorption pumps by coating the cold head with highly adsorbing materials such as activated charcoal or a zeolite.

Kinetic energy that they stay attached to the cold surface by weak intermolecular forces, resulting in significantly higher molecular concentration on the surface than in the gas phase. This phenomenon is called physical adsorption or physisorption. Gas particles impinging on a surface of sufficiently low temperature lose so much of their incident The amount of molecules that can be accumulated depends on a number of physical factors such as temperature of gas and surface, physicochemical properties of gas and surface, microscopic roughness of the surface, etc. [1][2][3]

Chapter 2

Project Details and Methodology

2.1 Project Title

Monte Carlo Approach for Transmission Probability & Radiation Heat Load and CFD Analysis for Cryopump Application.

2.2 Description of Project Work

2.2.1 Molecular Flow Analysis

Most of work in Movak 3D is generation of geometry for cryopump with use of basic command like triangle, parallelogram, circle, ring, cone etc. Thus, using with 3D transformation command (CAD feature) complicated geometry can be generated efficiently. And transmission probability of cryopump is geometry dependency terms. By varying geometry feature optimize geometry such that cryopump produce maximum transmission probability and good amount of $80^{\circ}K$ to $90^{\circ}K$ temperature molecular gas particles striking on cryopanel. So objective is to create CAD model programming in MCL language for innovative geometry of cryopump for this condition.

2.2.2 Radiation Analysis

Radiation heat load is one of the primary heat load acting on cryopanel of the cryopump. Cryopanel heat load must be minimized. For that situation finding radiation heat load for single panel cryopump with using Monte Carlo Ray Tracing technique. And minimization of heat load acting on cryopanel.

2.2.3 Fluid Analysis

For cryopumping, liquid helium flow is such that it has uniform distribution in cryopanel geometry and maintain temperature of panel under $5^{\circ}K$. For that case simulated cryopanel fluid flow for Bubble Panel and seam welded cryopanel.

2.3 Methodology

- Understanding the project.
- Literature review of related research in field of fusion science and technology.
- Conclusion and summary of boundary condition for cryopump.
- Molecular flow analysis.
 - a. Understanding Movak 3D code.
 - b. Learn Programming language.
 - c. Modeling different type of geometry for cryopump.
 - d. Bench marking for transmission probability.
 - e. Finding optimum geometry for transmission probability and nearer to $80^{\circ}K$ - $90^{\circ}K$ temperature particle gas load for cryopanel.
- Radiation heat analysis.
 - a. Understanding Radiation heat transfer.

- b. Heat transfer by MCRT method.
 - c. Bench marking radiation heat load problem.
 - d. Finding radiation heat load on cryopump using MCRT approach.
 - e. Finding optimum condition for emissivity for minimization radiation heat load for cryopanel.
- CFD analysis
 - a. Understanding pressure drop and heat transfer for heat exchanger.
 - b. Learn Ansys Fluent.
 - c. Bench marking for fluid flow.
 - d. CFD flow analysis of cryopanel channel for fluid flow.
- Summary of project.

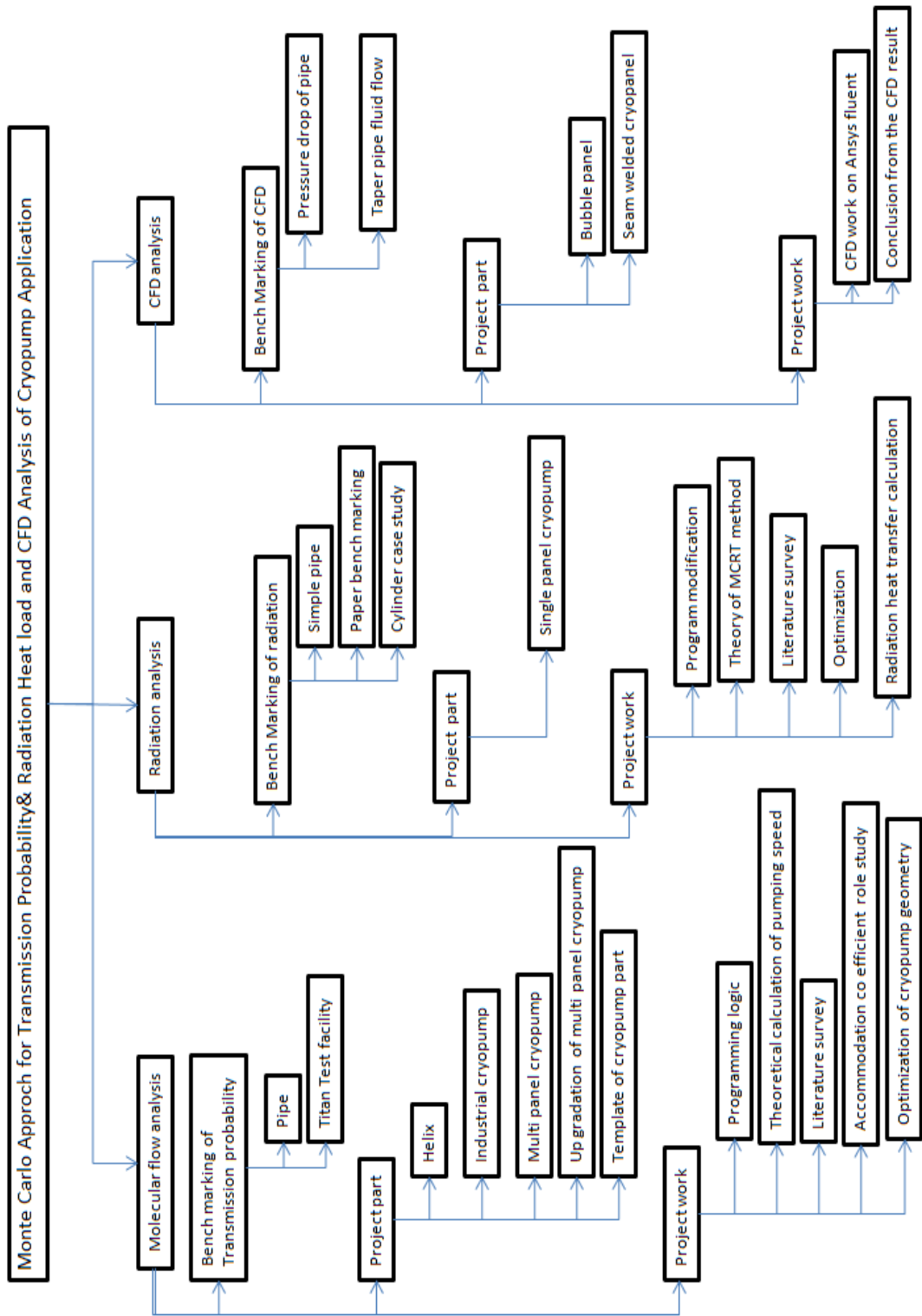


Figure 2.1: Project Detail Chart

Chapter 3

Literature Survey

3.1 Molecular Flow Analysis

3.1.1 Cryopump

A cryopump is defined as a vacuum pump which captures the gas by surfaces cooled to temperature below $120^{\circ}K$ [1].

- **Categories of Cryopump:-** Cryo condensation, Cryo sorption, Cryo trapping.
- **Heat Load Assessment:-** Solid conduction, Gaseous Heat conduction, Radiation heat transfer, Enthalpy transfer.
- **Cryopump Type:-** Bath type, Refrigerator cooled cryopump, Supercritical helium-cooled cryopumps, Alternative Cryopump.

3.1.2 Cryopump Design

The vacuum technological design of a cryopump aims to maximize the pumping speed S with in the existing cooling supply conditions and space limitations. The basic design shows that apart from the usual parameters such as temperature T , inlet cross section A , and the properties of the gas being pumped (mass M and gas constant R_o),

the only parameter left to adjust during design is the capture coefficient c , to which the pumping speed directly scales. The capture coefficient is given by the ratio of the actual pumping speed of the cryopump to the theoretical black hole pumping speed S_{id} and indicates the efficiency of the pump

$$S = c.S_{id} = c.A_{inlet} \cdot \sqrt{\frac{R_0.T}{2.\Pi.M}} \quad (3.1)$$

Thus, the pumping speed of a cryopump is a function of the geometry of its internal structures, the molecular weight M of the gas being pumped, and temperature. The latter effects are summarized by an overall sticking probability α (the number of particles sticking to the cryosurface related to the number of particles impinging on it) characterizing the overall gas-surface interaction. By this phenomenological approach, the first-order influences of geometry (summarized by ω) are separated from the second-order influences of gas-surface interaction (summarized by α). For the simplified case of parallel arrangements of the panel and the baffle, as typical for commercial refrigerator cryopumps, we have the following simple expression:

$$\frac{1}{c} = \frac{1}{\alpha} + \frac{1}{\omega} - 1 \quad (3.2)$$

Because of this geometry influence, it is not easy to scale the pumping speed from one geometry to another. The arrangement of cryopanel and shields is then rather

Table 3.1: Comparison Of Initial (Zero Gas Load) Sticking Probability for Nuclear Fusion Relevant Gases at Different Temperature

Temperature(K)	He	H ₂	D ₂	T ₂
5	0.35	0.6	0.9	1.0
	0.25			
7	0.17	0.5	-	1.0
12	0.03	0.3	0.85	-

complex so that the application of the simplified to estimate the capture coefficient is

no longer justified. In this case, Monte Carlo simulations of the pump interior have to be performed to calculate the capture coefficient. So for designing of cryopump Monte Carlo simulation is key tool[1][4][21].

3.1.3 Thermal Accommodation

Thermal Accommodation Coefficient

A molecule gas particle reaching a surface “accommodates to that surface” to a certain extent which is described by the accommodation coefficient. For example the accommodation coefficient for energy is defined as

$$\alpha = \frac{T_{particle,initial} - T_{particle,final}}{T_{particle,initial} - T_{wall}} \quad (3.3)$$

When the particle is remitted from the surface it has partially lost its previous properties as described by several accommodation coefficients for the several physical quantities for that particle-surface combination[16][18][27]. There are usually different accommodation coefficients for kinetic energy and momentum. The accommodation coefficients depend on all details of the collision such as

- Type of particle onto type of surface.
- Incident angle.
- Surface roughness.
- Particle.

Generally for cooled component thermal accommodation coefficient is 0.5 and 300K component thermal accommodation coefficient is 0.2[14][15].

3.1.4 Transmission Probability

Transmission Probability is defined as gas molecules finally reaching the absorber surface to those entered from the entrance aperture[3][22].

$$K = \frac{N_{absorber}}{N_{total}} = \frac{N_{absorber}}{N_{absorber} + N_{leave}} \quad (3.4)$$

3.1.5 Various Approach for Pumping Speed

Various approach to calculate pumping speed and thermal load from particle flux and radiation at molecular flow condition several approach is possible[8][20].

- Scaling from existing pump systems and from literature data for conductance of various vacuum components.
- The method of angular coefficients.
- The integral-kinetic method.
- The Monte Carlo method.

3.1.6 Monte Carlo Simulation

- The Monte Carlo computer simulation described in this article allows the user to conduct calculations of the pumping speed and condensate distribution of the given cryopump design with good precision.
- The program developed allows one to find the influence of the accumulated deposit on the sticking coefficient for the given pump configuration.[5]
- The results show that this model can be applied to predict the performance of new cryopump designs and to evaluate their features.[9][10]
- Quantitative and qualitative results are produced and both can be used to compare design alternatives.

3.1.7 Monte Carlo Simulation for Chevron Baffle Performance

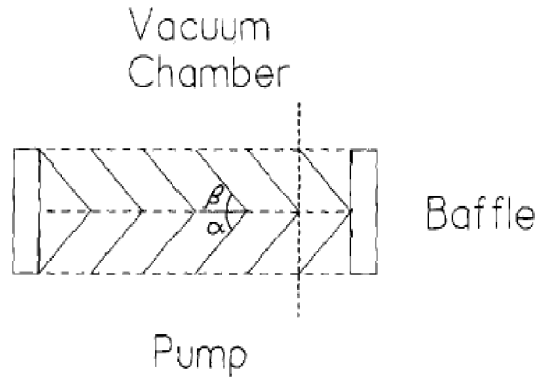


Figure 3.1: Chevron Baffle

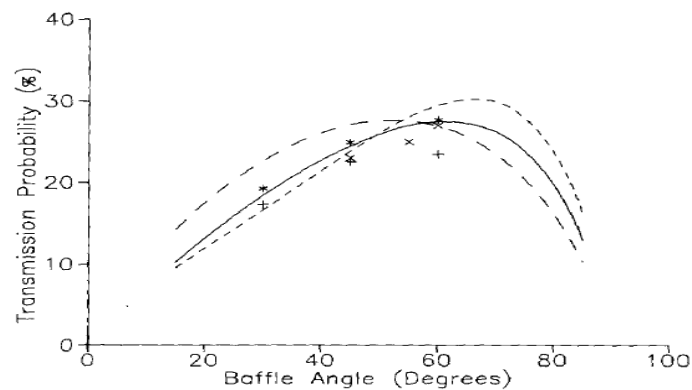


Figure 3.2: Result For The Three Baffle Configurations as a Function of Baffle Angle α . Solid Line, Chevron Configuration, Short Dashed Line, Offset Configuration; Long Dashed Line, Offset Configuration With β fixed At 90° , + Measured, * Calculated For Chevron Baffle

Monte carlo calculation for chevron baffle indicate that the optimum angle for the placement of the plates in a chevron diffusion pump bath He is 60° , and that a different configuration, the offset configuration, allows for faster pumping in a typical arrangement when used at 65° [7].

3.2 Radiation Analysis

3.2.1 Radiation

Radiation heat transfer is concerned with the exchange of thermal radiation energy between two or more bodies. No medium need exist between the two bodies for heat transfer to take place. The heat transferred into or out of an object by thermal radiation is a function of several components. These include its surface reflectivity, emissivity, surface area, temperature, and geometric orientation with respect to other thermally participating objects. In turn, an object's surface reflectivity and emissivity is a function of its surface conditions (roughness, finish, etc.) and composition.

Since most solid bodies are opaque to thermal radiation, we can ignore the transmission component and write,

$$1 = \varepsilon_{reflected} + \varepsilon_{absorbed} \quad (3.5)$$

To account for a body's outgoing radiation (or its emissive power, defined as the heat flux per unit time), one makes a comparison to a perfect body who emits as much thermal radiation as possible. Such an object is known as a black body, and the ratio of the actual emissive power E to the emissive power of a black body is defined as the surface emissivity ε ,

$$\varepsilon = \frac{E}{E_{blackbody}} \quad (3.6)$$

The heat emitted by a black body (per unit time) at an absolute temperature of T is given by the Stefan-Boltzmann Law of thermal radiation,

$$\dot{Q} = A.\sigma.T^4 = A.E_{blackbody} \quad (3.7)$$

where \dot{Q} has units of Watts, A is the total radiating area of the black body, and σ is the Stefan-Boltzmann constant.[25]

3.2.2 Gray Body Radiation Heat Transfer

Bodies that emit less thermal radiation than a black body have surface emissivity less than 1. The net heat transfer from a small gray body at absolute temperature T with surface emissivity to a much larger enclosing gray (or black) body at absolute temperature T_e is given by,

$$\dot{Q} = \epsilon \cdot A \cdot \sigma (T^4 - T_e^4) \quad (3.8)$$

The above equations for black bodies and gray bodies assumed that the small body could see only the large enclosing body and nothing else. Hence, all radiation leaving the small body would reach the large body. For the case where two objects can see more than just each other, then one must introduce a view factor F and the heat transfer calculations become significantly more involved. The view factor F_{12} is used to parameterize the fraction of thermal power leaving object 1 and reaching object 2. Specifically, this quantity is equal to,

$$\dot{Q}_{1-2} = A_1 \cdot F_{12} \cdot \epsilon_1 \cdot T_1^4 \quad (3.9)$$

Likewise, the fraction of thermal power leaving object 2 and reaching object 1 is given by,

$$\dot{Q}_{2-1} = A_2 \cdot F_{21} \cdot \epsilon_2 \cdot T_2^4 \quad (3.10)$$

To decrease the radiation heat load of the cryopanel is considered to be necessary for the design of cryopumps. In general, a radiation baffle is mounted between the cryopanel and the heat source. The radiation baffle absorbs the majority of the radiated heat load. However, the motion of molecules to be pumped is baffled and the pumping speed is lowered at the same time. Therefore the selection of a good radiation baffle is a very important issue for the economical operation of the cryopump[25].

Role of The Radiation Baffle in a Cryopump

- Preventing the radiation heat loads from the vacuum chamber wall from falling directly onto the cryopanel.
- Pumping gas. The radiation baffle can remove hot gases-hotter than the boiling point of water emitted from the atmosphere and a room temperature vacuum enclosure, such as water vapor and carbon dioxide, etc.
- Cooling uncondensed gas at the $77\text{ }^{\circ}\text{K}$ baffle temperature, for instance Argon, Oxygen and Nitrogen, etc.[28]

Main Considerations in The Design of the Radiation Baffle

- The baffle should be of a maximal molecular pass through transmission coefficient.
- For the sake of decreasing the temperature difference between the first stage of the cold head and the baffle as soon as possible, the first stage of the cold head and the baffle should be kept in good contact in order to lower heat conduction
- The baffle should reduce the thermal transmission from the vacuum chamber wall at room temperature in order to act as a good heat screening. Therefore the baffle should be enclosed by photons and be made opaque to thermal radiation.[28]

3.3 Fluid Analysis for Cryopanel

Bao Min, Fu Xin, Chen Ying observed that With the development and use of CFD, it is possible to examine and predict a valve characteristic and to optimize the geometry before it is manufactured. The simulation result could be helpful for valves and hydraulic component design. The results of simulation have shown that modification of the in-and outlet area is the most successful way to improve the valve with regard to reduce the pressure loss.[29]

A. Witry And M. H. Al-Hajeri And Ali A. Bondok observed from CFD simulation of dimple plate heat Exchanger design that attention should also given to coolant flow velocity inside the plate. thermal performance of heat exchanger an important role in cooling system and all over associated system. CFD result obtain for patterned plate heat exchanger using the CFD code. Result shows tremendous level of possible performance improvement on both side of heat exchanger.[30]

Fluid distribution in cryopanel is very important for effective heat transfer surface wall and minimum pressure loss.

Chapter 4

CAD Work in Geometric Modeling in Movak 3D

4.1 Movak 3D Programming

Movak 3D uses modeling preprocessor command circle,parallelogram,triangle,ring,cone type of surface for geometric modeling.So for complicated geometry effective modeling is done by CAD utilization this programming language offers nevertheless the following advantages:

- Variables may be defined, based on which that model geometry may be laid out.
- Other variables may be calculated from the predefined variables using typical mathematical functions
- Loop constructs are allowed: This is very useful for creating several times the same shape.
- The existence of variables is the basis for optimization runs with MOVAK3D.

The use of MCL can be very efficient in such cases, either if complex trigonometrical function are often used in the creation of a model, or when a model shall be optimized . For optimization calculations, the same model with slight changes must be reproduced and then put into a Monte Carlo simulation with MOVAK3D.

4.2 Programming Step and its Meaning for Main Component of Cryopump

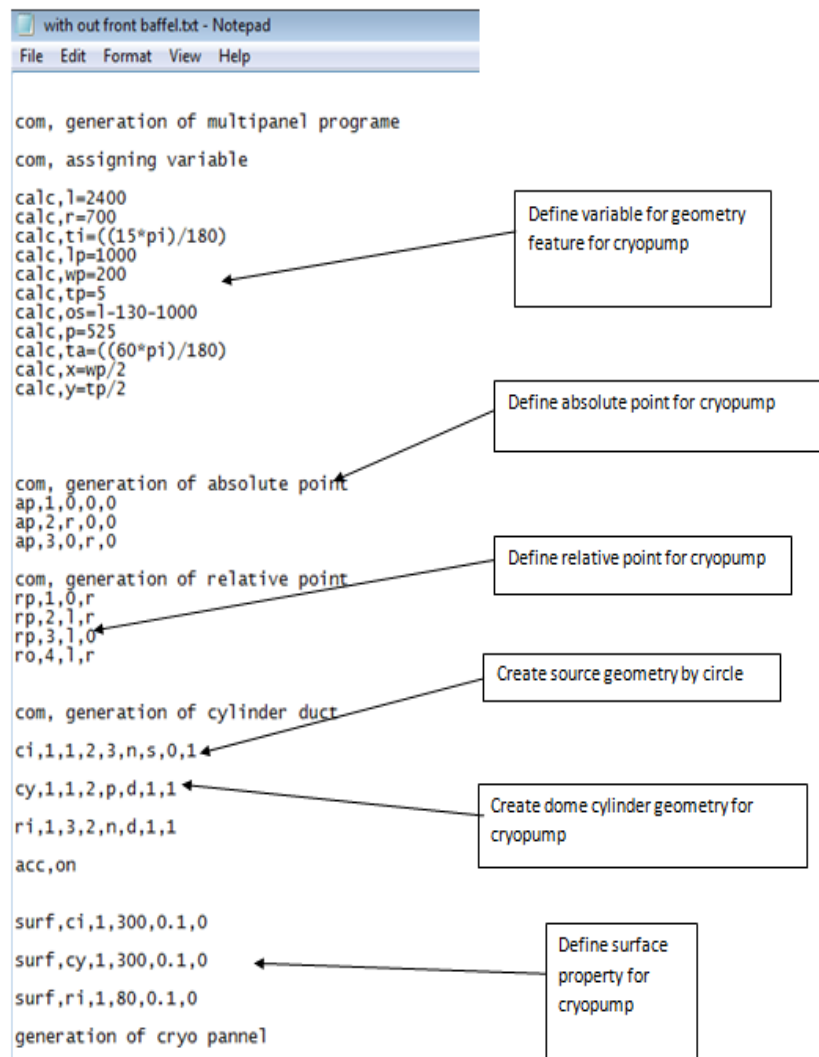


Figure 4.1: Program for Defining Variable, Title, Absolute Point, Relative Point, Surfaces, Surface Property for Outer Surface.

```

with out front baffel.txt - Notepad
File Edit Format View Help
generation of cryo panel

calc,npa=0
repeat,i,1
calc,thi=(ti*i)
calc,t=((thi)+(pi/4))
calc,x1=((p)*(cos(thi)))
calc,y1=((p)*(sin(thi)))
calc,p1=1+i*10
calc,p2=2+i*10
calc,p3=3+i*10
calc,p4=4+i*10
calc,p5=5+i*10
calc,p6=6+i*10
calc,p7=7+i*10
calc,p8=8+i*10
calc,q1=(x*(cos(t)))-(y*(sin(t)))
calc,q2=(x*(sin(t)))+(y*(cos(t)))
calc,q3=(x*(cos(t))-((-y)*(sin(t)))
calc,q4=(x*(sin(t))+((-y)*(cos(t)))
calc,q5=(-x*(cos(t))-((-y)*(sin(t)))
calc,q6=(-x*(sin(t))+((-y)*(cos(t)))
calc,q7=(-x*(cos(t)))-(y*(sin(t)))
calc,q8=(-x*(sin(t)))+(y*(cos(t)))

com,*****generate points
ap,p1,q1+(x1),q2+(y1),os
ap,p2,q3+(x1),q4+(y1),os
ap,p3,q5+(x1),q6+(y1),os
ap,p4,q7+(x1),q8+(y1),os
ap,p5,q1+(x1),q2+(y1),os+lp
ap,p6,q3+(x1),q4+(y1),os+lp
ap,p7,q5+(x1),q6+(y1),os+lp
ap,p8,q7+(x1),q8+(y1),os+lp

pa,npa+1,p1,p4,p2,p3,p,a,0,1
pa,npa+2,p5,p6,p8,p7,p,a,0,1
pa,npa+3,p8,p7,p4,p3,p,a,0,1
pa,npa+4,p5,p1,p6,p2,p,a,0,1
pa,npa+5,p8,p4,p5,p1,p,a,0,1
pa,npa+6,p6,p2,p7,p3,p,a,0,1

surf,pa,npa+1,4.5,0,0
surf,pa,npa+2,4.5,0,0
surf,pa,npa+3,4.5,0,0
surf,pa,npa+4,4.5,0,0
surf,pa,npa+5,4.5,0,0
surf,pa,npa+6,4.5,0,0

calc,npa=npa+6
until,24

```

Define absolute point and create 24 cryopanel by using 3D transformation mathematical formula put in form of coding

Defining surface property for cryopanel

Figure 4.2: Programming Step for 24 Cryopanel Generation. It Include 3D Transformation Mathematical Logic and set in Programm Line Command.

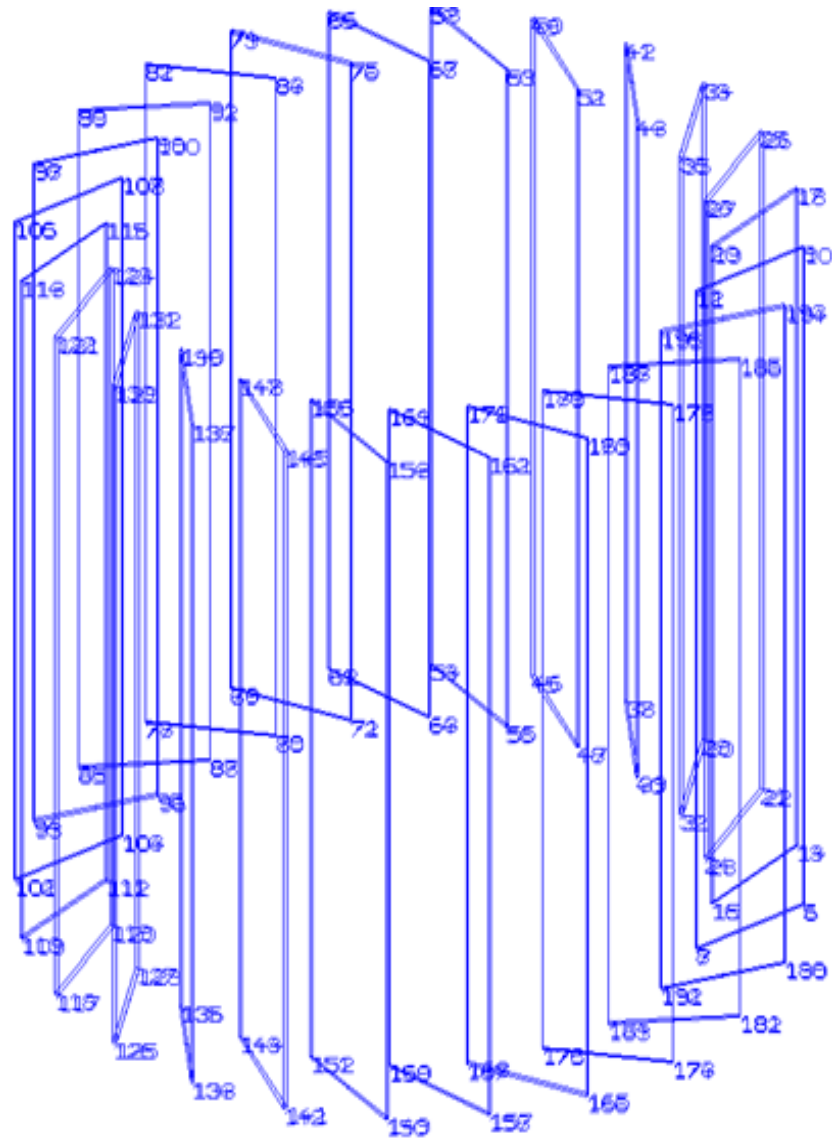


Figure 4.3: Movak 3D Generated Model of 24 Cryopanel (result of Program Logic).

```

test program1.txt - Notepad
File Edit Format View Help
until,24

calc,pitch=70

calc,cno=0
calc,lb=70
calc,os1=1-130-1000-70
calc,angle=45

com, generation of baffle

calc,cyn=1
repeat,i,1

calc,p1=5+(i-1)*4
calc,p2=6+(i-1)*4
calc,p3=7+(i-1)*4
calc,p4=8+(i-1)*4
com, generation of baffle point
rp,p1,os1+pitch,300
rp,p2,os1+pitch+(70),300+(70)
rp,p3,os1+pitch+(70)+10,300+(70)
rp,p4,os1+pitch+10,300

co,cno+1,p1,p2,n,d,1,1
co,cno+2,p4,p3,p,d,1,1

cy,cyn+1,p1,p4,p,d,1,1
cy,cyn+2,p2,p3,n,d,1,1

|
surf,co,cno+1,80,0.1,0
surf,co,cno+2,80,0.1,0
surf,cy,cyn+1,80,0.1,0
surf,cy,cyn+2,80,0.1,0

calc,cno=cno+2
calc,os1=os1+pitch

calc,cyn=cyn+2

until,15

```

Create 15 baffles using repetitive pattern 3D transformation of lower baffle geometry

Figure 4.4: Defining 15 Baffle of Cryopump, Which is Created by Using Repeat Loop and Increment of Distance in The Code.

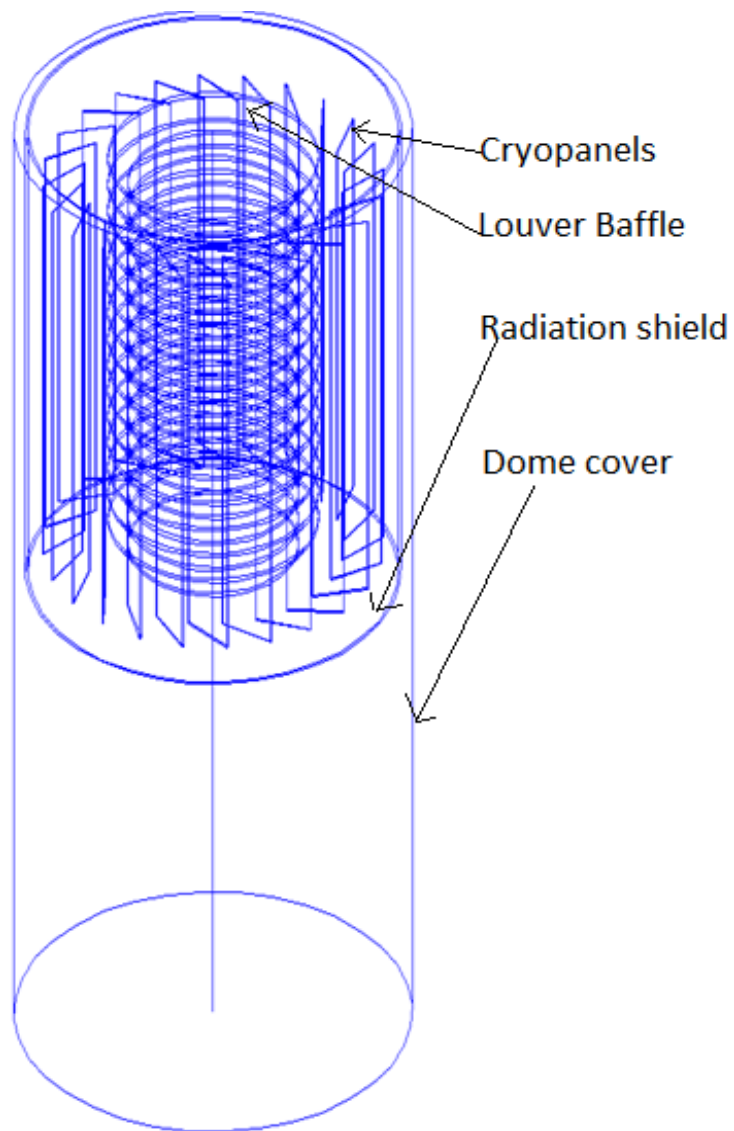


Figure 4.5: Final CAD Model Done In Cryopump due to Programming of Dome, Cryopanel and Louver Baffles.

Chapter 5

Molecular Flow Analysis

Molecular regime is calculating by the Knudsen number (Kn). The Knudsen number is defined as $Kn = \lambda/D$, where λ is the mean free path length of a molecule and D is a typical size of a model. If the Knudsen number is much larger than 1 then you are working in a molecular regime. This means, that molecules travel from wall to wall but never hit onto another molecule.

Tokamak gas load is in form is high Knudsen region. In this range molecular flow cannot analyzed by CFD due to complete failure of Navier-Stokes equation. In that range flow can be simulated by Monte Carlo simulation. DSMC and TPMC method is used for High Knudsen flow region.

In the case of transmission probability can be analyzed by TPMC method. Movac 3D software is based on TPMC method. But in case of following condition in TPMC code generation for complicated geometry is very difficult task. For that case geometry creation of complicated geometry requires extensive knowledge of CAD.

5.1 Movak 3D

Description of a vacuum system with MOVAK3D (basis-knowledge) and simulation with MOVAK3D requires three processing steps[27]:-

5.1.1 Geometric Modeling of the Apparatus

- The apparatus may be modeled with triangles and parallelograms in three-dimensional space. this allows the creation of an arbitrary physical shape.
- In addition, rotationally symmetric parts may be attached to the triangles and parallelograms, i.e. cylinders, cones, rings, and circles.
- To connect these rotationally symmetric parts to the triangles and parallelograms MOVAK3D offers connection elements, i.e. a square with hole, a hexagon with hole, an octagon with hole and a circle.

5.1.2 A Surface Property Assignment

The property value assigned to each surface specifies the type of a surface with respect to its physical behavior. The following physical behaviors (properties) are offered (one choice for each surface).

- Source: The emission distribution of particles with respect to angles and distribution along the surface may be chosen.
- Also the attributes “ideally absorbing” or “diffusely reflecting” must be selected.
- An absorber, which also may scatter according to a cosine distribution.
- A diffuse scatterer which emits according to a cosine distribution.
- A mirror like reflector: This type is employed to model photons (for example radiative heat transfer). Also this type is applicable for problems where sym-

metry considerations allow to split the problem into identical subsystems which can be computed more efficiently.

- Control surfaces: These surfaces are used to reduce the amount of computer time needed to track particles and to calculate pressures at specific locations in the model.

5.1.3 Running a Monte-Carlo Simulation

In a Monte-Carlo simulation MOVAK3D proceeds as follows:- It randomly chooses a source surface and emission coordinates for a particle. Next, the emission direction is randomly chosen. Usually, the emitted particle is given unity weight. Now, the wall (surface) which is hit by the particle is computed. Also the exact coordinates (on the surface) where the particle hits the surface are evaluated. The flight from wall to wall is assumed to follow straight lines. This assumes that gravity is negligibly small and that pressure is sufficiently low so that intermolecular collisions of molecules are negligibly rare events. The destiny of the particle depends on the physical type (i.e. the surface property) of the surface hit. An absorber or reflector surface scatters the particle. Scattering may be diffuse, mirror-like reflection or according to an accommodation model.

5.1.4 Geometric Modeling Base

Point :- Absolute Point, Relative Point

Surface :- Triangle, Rectangle, Cylinder, Ring, Circle, Cone

Property :- Surface Orientation (Positive, Negative), Reflection coefficient, Temperature, Accommodation coefficient, Source, Absorber

CAD Technique for Modeling Movak 3D Geometry

- Mathematical function for geometric modeling.
 - a. sin , asin- sin and arcsin with angles in radians.
 - b. cos, acos - cos and arccos with angles in radians.
 - c. tan, atan - tan and arctan with angles in radians.
 - d. ln, exp - natural logarithm, exponential function.
 - e. log10, pow10 - logarithm with basis 10, power with base 10.
 - f. sqrt, sqr - square root, square.
 - g. abs - absolute value.
 - h. round - rounding down or up to the next integer whichever is closer.

- General command.
 - a. Calc:-define variable.
 - b. Clear:- clear all data.
 - c. Com:-for comment.
 - d. end end program me.
 - e. go to:- go to specific location.
 - f. if :- for condition statement.
 - g. label:- create label.
 - h. Repeat:- repeat loop execution.

5.2 Experimental Verification for Movak 3D Transmission Probabiliy Result

5.2.1 Verification of Transmission Probability for Pipe Geometry with Literature and Movak3D Simulation

Theory for Transmission Probability

Davis and Levenson et al.(1960,1963) used the Monte Carlo calculation method, for determining the conductance of simple and complex shapes. Davis Levenson and Millerson use the conductance C_0 of the aperture to the geometrical configuration being investigated, as their references. The computed and measured conductance C is related to by the probability factor P_r

$$\frac{C}{C_0} = P_r \quad (5.1)$$

The assumptions made in the calculation and the experimental conditions provided are:-

- Steady molecular flow exists.
- Molecules enter the inlet aperture uniformly distributed over its surface.
- The geometry under study connects effectively large volumes.
- The probability of the molecule entering a solid angle is proportional to the cosine of the angle to the normal to the surface of the opening.
- The walls are microscopically rough, so that molecules are diffusely reflected according to the cosine law.

The first geometry investigated is one which can also be determined by simple calculation. It is that of tube of circular cross section, where the conductance can be calculated.the value of Pr is in this case,

$$\frac{C}{C_0} = Pr \quad (5.2)$$

$$Pr = C/C_0 = (3.81/2.86)[D^3/(L + 1.33D)](1/D^2) \quad (5.3)$$

$$\begin{aligned} &= \frac{4}{3} * D/[L + \frac{4}{3}D] \\ &\approx \frac{4}{3}(\frac{D}{L})K'' \end{aligned}$$

The Monte Carlo computation and experimental results in good agreement with eqn especially if K' is used instead of K'' [22]

Where

$$K' = \frac{15(\frac{L}{D}) + 12(\frac{L}{D})^2}{20 + 38(\frac{L}{D}) + 12(\frac{L}{D})^2} \quad (5.4)$$

Pipe Modeling in Movak 3D

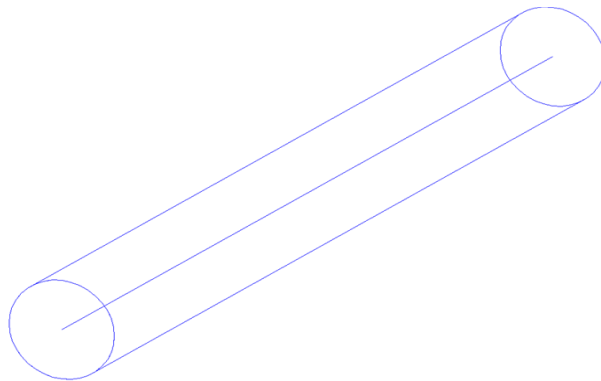


Figure 5.1: Pipe Model in Movak 3D

Program for Pipe Model

Cylinder:-

```
Title, simple pipe model
Com, *****define title name*****
Ap,1,0,0,0
Ap,2,10,0,0
Ap,3,0,10,0
Com, *****absolute point is defined *****
Ci,1,1,2,3,n,sw,0,1
com, *****circle is defined *****
rp,1,0,10
rp,2,100,10
rp,3,100,0
Com, *****relative point is defined *****
Cy,1,1,2,p,d,1,1
Com, *****cylinder is defined *****
ri,1,2,3,n,a,0,1
Com, ***** ring is defined *****
End, no save
Com, ***** end of the program*****
Exit
```

Simulation of Particle Trajectory

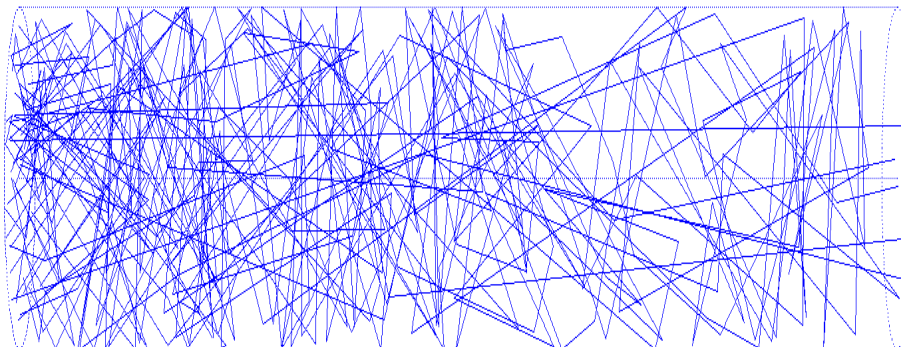


Figure 5.2: Particle Simulation in Pipe

Simulation Result

Sr No	D=10	L=100	L/D	k'	Pr theoretical	Movak 3D
1	10mm	100mm	10	0.84375	11.25%	10.87%
2	50mm	100mm	2	0.541667	36.11%	35.681%
3	400mm	600mm	1.5	0.475962	42.3076%	41.6%
4	600mm	700mm	1.16667	0.419421	47.9338%	47.67%

Table 5.1: Comparison with Movak 3D Simulation Result with Theoretical Correction Factor Result

Summary

Movak 3D simulation result is very good agreement of theoretical result and experimental.

5.2.2 Transmission Probability Experimental Bench Marking (Titan Test Facility)

In experiment, Karlsruhe Research Center determine sticking coefficient for helium and helium containing mixtures on activated carbon under liquid helium cooling condition.

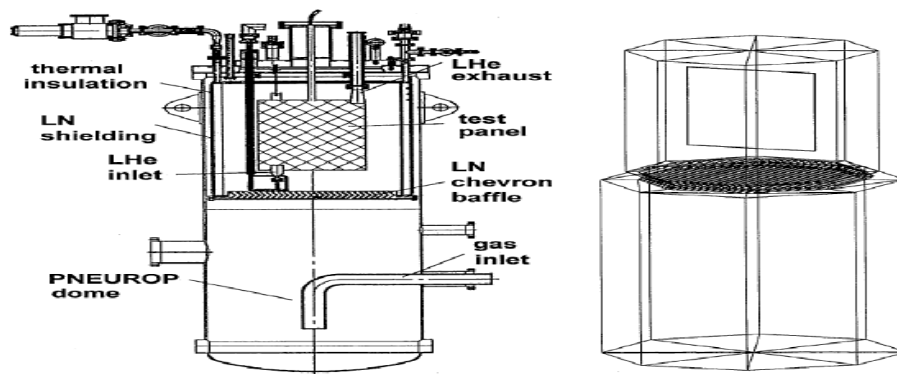


Figure 5.3: Titan Test Facility: Cross-Section and Monte Carlo Model

The tests were performed in the upgraded UHV test facility TITAN shown in figure 5.3

The capture probability c of the pump structure results directly from the measurement and can be calculated using the average gas velocity from the Maxwellian distribution: $c = \frac{S}{A_b \cdot V_x}$. The capture probability is a function of the sticking coefficient of the charcoal coated panel and, via V_x , also of the molecular mass of the gas to be pumped. The reference temperature is chosen to be $273.15 \text{ }^\circ\text{K}$. For a system of two components (baffle and panel) connected in series, the sticking coefficient a can be derived from the equation $\frac{1}{a} = \frac{1}{c} - \frac{1}{w} + 1$, provided the transmission probability w of the quilted panel, shielded by the chevron baffle, is known. This has been calculated by means of a Monte Carlo method applying the MOVAK3D Code. (No gas-gas interactions, no velocity distribution considered). The facility geometry structure, exhibiting four characteristic elements (the PNEUROP dome, the baffle, and the

cryopanel, embedded into the 80 K volume) was adequately modeled, representing cylindrical surfaces as prisms with an octagonal cross-section. It was proved that this approximate treatment had no significant influence on the final results. The Monte Carlo value for the transmission probability ω of the chevron baffle was determined to be 0.190, which corresponds very well to literature values. The combined transmission probability ω of the shielded panel was calculated to be 0.11 in our model. It is somewhat smaller than ω because the panel is not orthogonal to the main flow direction. This theoretical value is in agreement with the experimental result of 0.14 (within the limits of maximum measurement uncertainty), determined from experiments with nitrogen, whose sticking coefficient at LHe-cooled charcoal is known to be unity.[12][13]

Approximate Dimensioning of Titan Test Facility

- Cryopanel:- Length = 500mm, Width = 350mm, Thickness = 10mm.
- Baffle:- Chevron baffle angle = 106° , Baffle dia = 527mm. No of baffle = 28.
- Upper shield dimension:- Diameter = 0.7m, Length = 2.2m.

Programming Step Algorithm Of Movak 3D

- Creation of circle.
- Creation of center left baffle.
- Create 13 baffle pattern in left direction.
- Create 14 baffle pattern in right direction.
- Creation of cylinder for baffle.
- Creation of connecting duct of circle and baffle.
- Creation of cryopanel.

- Creation of rear side duct.

Geometric Modeling for Titan Test Facility

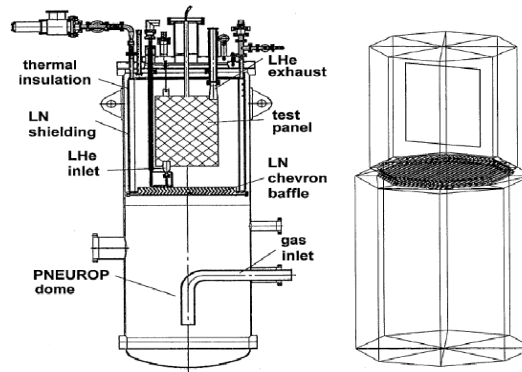


Figure 5.4: Titan Test Facility Modeling In Movak 3D In Research Paper

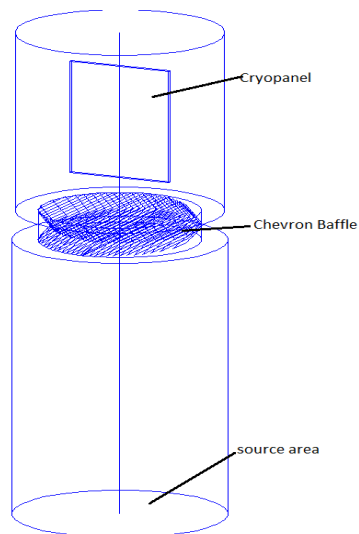


Figure 5.5: Titan Test Facility Modeling in Movak 3D for Validation

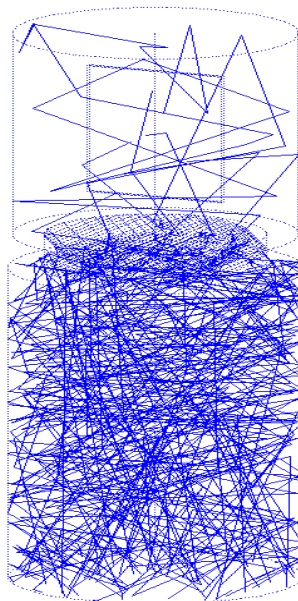


Figure 5.6: Titan Test Facility Modeling Particle Trajectory for 50 Particle

Sr no	source partical	Absorber	T.P	T.P in paper	Paper experiment result(T.P)*
1	100	10	0.1	0.167	0.14
2	1000	107	0.107	0.167	0.14
3	10000	1112	0.1112	0.167	0.14
4	100000	11105	0.11105	0.167	0.14
5	1000000	110699	0.110699	0.167	0.14

Table 5.2: Titan Test Experimental Validation Compare With Movak 3D Code Result

Summary

Experimental result for transmsion probabiliy at cryogenic temperature is very good agreement with Movak 3D simulatin result.

5.3 Project Work Done

5.3.1 Back Ground of Work

- Various geometry for such suitable condition must be study for maximum amount of 80°K temperature particle striking on cryopanel, minimize radiation heat load and good amount of transmission probability.
- For this situation we consider that a thermal accommodation criterion for fusion reactor exhaust gas load situation is 0.1. accommodation co efficient.
- Source of inlet of geometry is consider as uniform source, and particle is diffuse scatter after cullied with wall of geometry.
- Absorber completely absorb particle in absorber area,Reflection co efficient for diffuse scatter wall is consider as 1,And reflection co efficient for source and absorber is 0.
- Modeling of geometry is done with basic geometry element like circle, cylinder cone, ring, and triangle.Modeling of program is written in txt doc file.
- After completion of file compile with Movak solver and load with in Movak 3d code.And simulate trajectory of molecular within define geometry.
- After this completion of this analysis we can get data of transmission probability of cryopump geometry and amount of 80K temperature particle striking on cryopanel.

5.3.2 Industrial Cryopump

Dimension of Industrial Cryopump

- Source area:- Radius = 250mm.
- Radiation shield:- inner radius = 230mm, Length = 550mm, thickness = 10mm.
- Baffle:- thickness = 1mm, width = 40mm, angle = 45, no = 5.
- Conical Cryopanel:- cone radius 1 = 16mm, cone radius 2 = 200mm, Length = 500mm.
- Dome:- radius = 250mm, Length = 1000mm.

Thermal Boundary Condition for Industrial Cryopump

Sr No	Component name	Temperature	Thermal Accommodation Coefficient
1	source	300°K	0
2	Dome	300°K	0
3	Radiation shield	80°K	0.4
4	Louver Baffle	80°K	0.4
5	conical cryopanel	4.5°K	0.4

Table 5.3: Movak3D boundary condition for industrial cryopump

Movak 3D Modeling Surfaces for Industrial Cryopump

Sr No	Component Name	No of Used
1	circle	1
2	cylinder	4
3	ring	5
4	cone	13

Table 5.4: Movak 3D surface utilization for industrial cryopump CAD modeling

Movak Modeling Algorithm for Industrial Cryopump

- Create circle by define absolute point.
- Create cylinder for dome using relative point.
- Create radiation shield.
- Creation of louver baffle.
- Creation of cold head.
- Creation of cryopanel.
- Run for 10,00,000 particle.
- Get Transmission Probabiliy and 80°K-90°K particle for it.

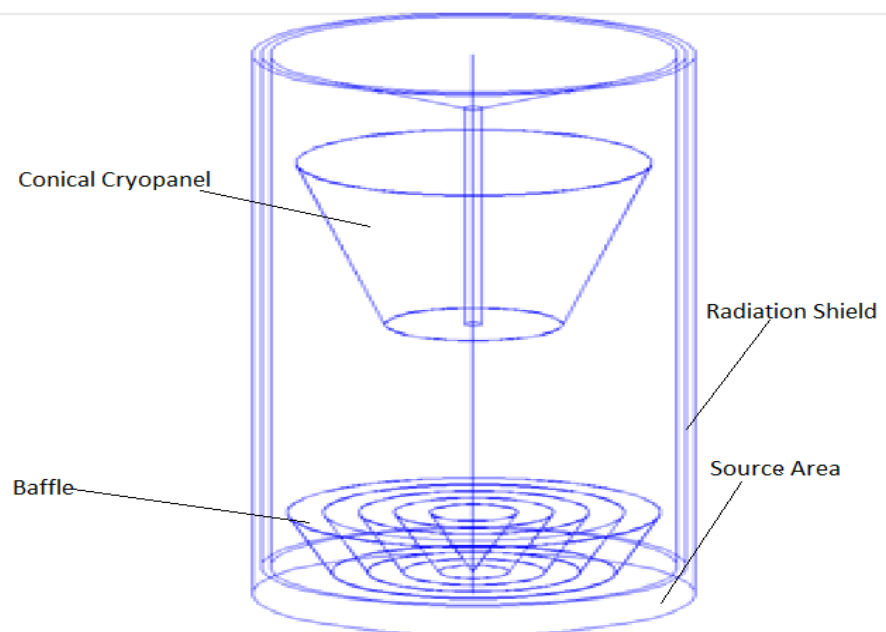


Figure 5.7: Industrial Cryopump Movak 3D Modeling

Simulation Result Output From Movak 3D for Transmission Probability

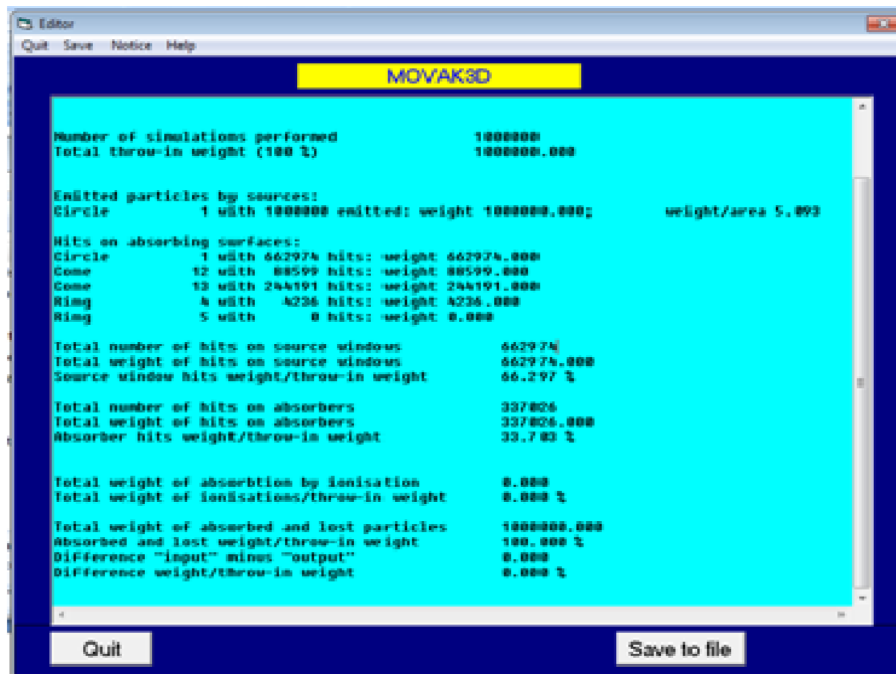


Figure 5.8: Transmission Probability Result for Industrial Cryopump

Summary

In industrial cryopump Transmission probability is 35.70%. But there is more probability of higher temperature gas particles striking on the cryopanel.

5.3.3 Helix Geometry

Dimension of Helix

- Circle:- Radius = 435mm.
- Cylinder:- Length = 550mm.
- Ring:- radius = 450mm.
- Helix
 - No = 16.
 - Angle of twist = vary from 10 to 360°.

Thermal Boundary Condition for Helix

Sr No	Component name	Temperature	Thermal Accommodation Coefficient
1	source	300°K	0.1
2	pipe wall	80°K	0.1
3	absorber	4.5°K	0.1
4	Helix	80°K	0.1

Table 5.5: Thermal Boundary Condition for Temp and Thermal Accommodation for Helix

Movak 3D Modeling Surfaces for Helix

Sr No	Component Name	No of Used
1	circle	No
2	cylinder	1
3	ring	1
4	Triangle	890

Table 5.6: Movak 3D modeling surface utilization for helix.

Movak Modeling for Helix analysis

- Creat circle by define absolute point.
- Create cylinder using relative point.
- Create ring with help of relative point.
- Create helix by using triangle(this gromery is define by using combine 3D transformation and rotation mathematical function).
- Run for 10,00,000 particle.
- Get Transmission Probabiliy and 80°K - 90°K particle for it.

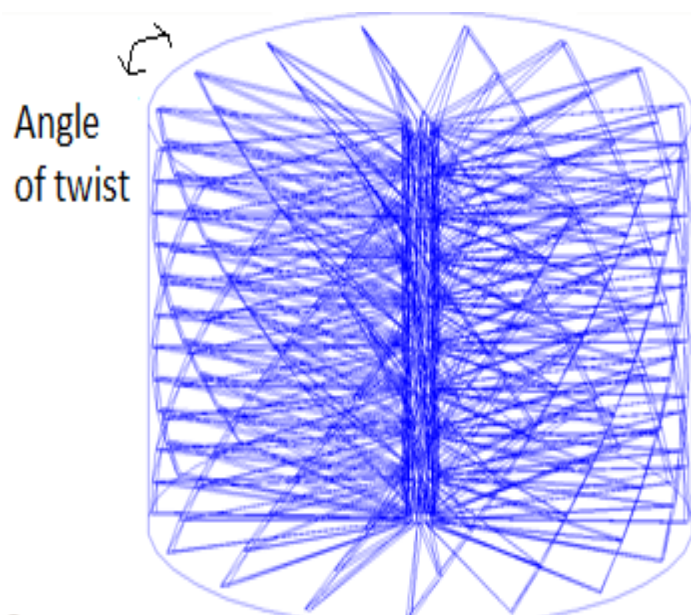


Figure 5.9: Helix Modeling in Movak 3D

Helix Reult for 80-90°K Particle and Transmission Probability

Sr No	Angle twist	T.P	80-90°K parti	Sr No	Angle twist	T.P	80°K parti
1	No blade	95.115%	0%	11	65°	42.67%	25.41%
2	0°	69.112%	5.24%	12	70°	40.44%	10.51%
3	10°	77.68%	4.09%	13	80°	30.762%	17.76%
4	20°	75.045%	2.62%	14	90°	26.27%	27.56%
5	30°	63.82%	2.76%	15	135°	14.19%	49.63%
6	40°	64.72%	2.57%	16	180°	10.44%	75.81%
7	45°	59.16%	12.13%	17	225°	7.89%	83.13%
8	50°	55.71%	15.4%	18	270°	6.61%	85.53%
9	55°	51.95%	20.53%	19	360°	6.06%	85.23%
10	60°	46.81%	26.93%				

Table 5.7: Helix Reult for 80-90°K Particle and Transmission Probability(*where parti=particle)

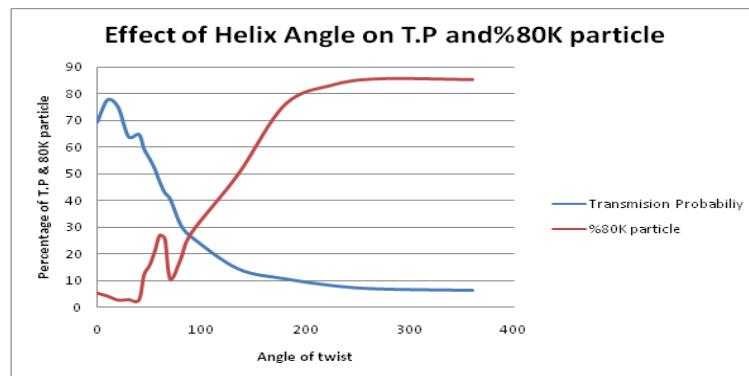


Figure 5.10: Chart For 80°K and TP Optimization

Summary

In Helix geometry 60° of twist is optimum angle of twist for for 80-90°K temperature gas particle and good amount of transmission probability.

5.3.4 Multi Panel Cryopump

Dimension Of Multi Panel Cryopump

- Source area:- Radius = 300mm
- Radiation shield:- radius = 650mm, Length = 1700mm, thickness=30mm
- Baffle:- thickness = 1mm, width = 450mm, angle = 7.5° , no = 9, pitch = 70mm
- Cryopanel:- width = 200mm, thickness = 10mm, Length = 1000mm, no = 16
- Dome:- radius = 720mm, Length = 2500mm

Thermal Boundary Condition for Multipanel Cryopump

Sr No	Component name	Temperature	Thermal Accommodation Coefficient
1	source	300°K	0
2	Dome	300°K	0
3	Radiation shield	80°K	0.1
4	Baffle	80°K	0.1
5	cryopanel	4.5°K	0.1

Table 5.8: Movak 3D Thermal Boundary Condition for Multipanel Cryopump

Movak 3D Modeling Surfaces for Multipanel Cryopump

Sr No	Component Name	No of Used
1	circle	1
2	cylinder	4
3	ring	7
4	cone	24
4	parallelogram	144

Table 5.9: Movak 3D Surface Utilization for Multipanel Cryopump

Movak Modeling Algorithm Step for Multipanel Cryopump

- Create circle by define absolute point.
- Create cylinder for dome using relative point.
- Create radiation shield.
- Creation of baffle(this thing is modify after modification 1 and 2).
- Creation of valve.
- Creation of cryopanel.
- Run for 10,00,000 particle.
- Get Transmission Probabiliy and 80°K particle for it.

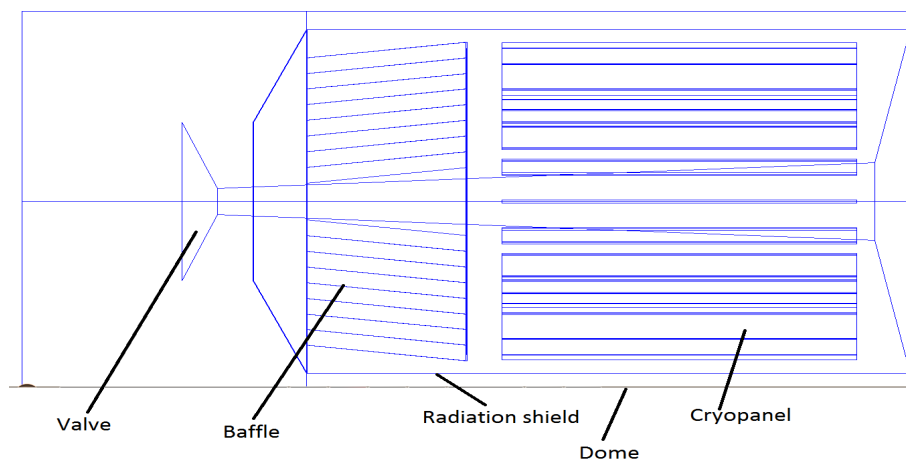


Figure 5.11: Multipanel Cryopump Movak 3D Modeling

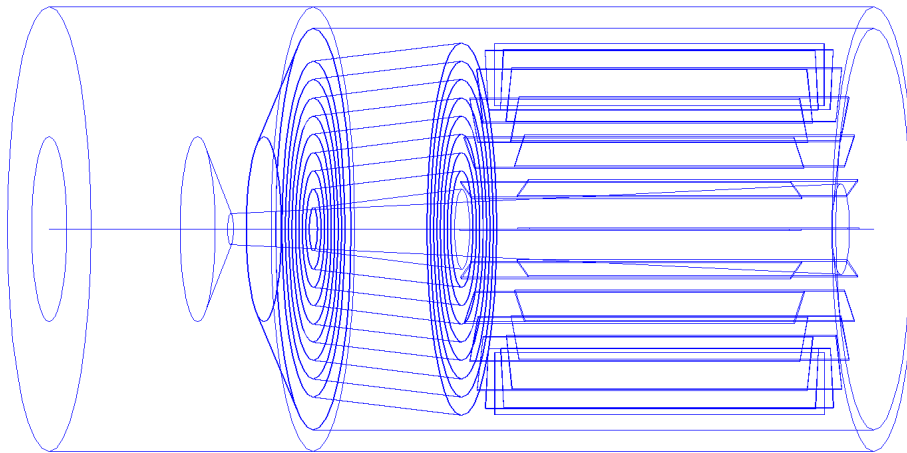


Figure 5.12: 3D View of Multipanel Design

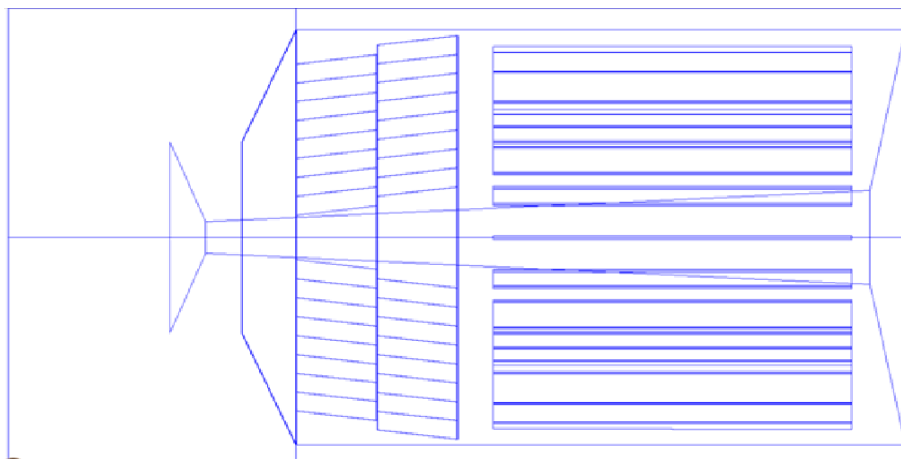


Figure 5.13: Multipanel Cryopump Modification 1 Movak 3D Modeling

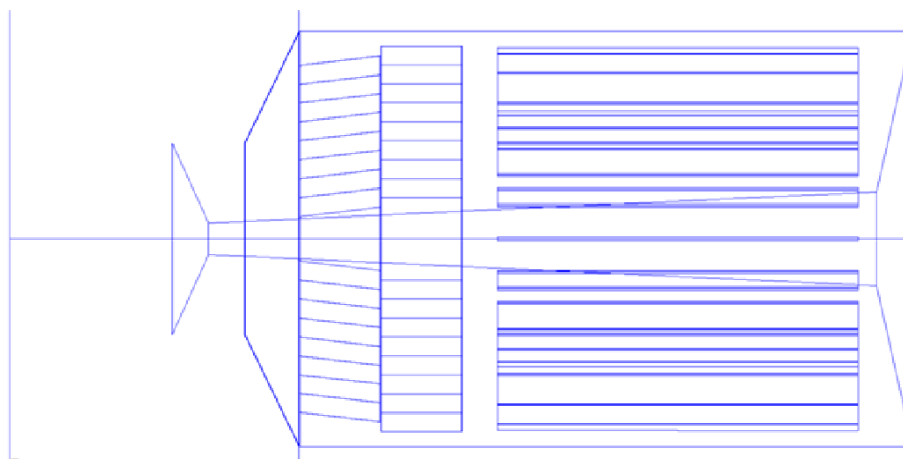


Figure 5.14: Multipanel Cryopump Modification 2 Movak 3D Modeling

sr no	Name	TP	80 ^o K-90 ^o K particle
1	Multi panel cryopump initial	35.83%	33.70%
2	Multipanel cryopump modification 1	35.936%	33.25%
3	Multipanel cryopump modification 2	35.913%	33.63%

Table 5.10: Movak 3D Result for Transmission Probability and 80^oK-90^oK Particle for Multipanel Cryopump

5.3.5 Tubing Multipanel Cryopump

Dimension Of Tubing Multipanel Cryopump

- Source area:- Radius = 300mm.
- Radiation shield:- Radius = 650mm, Length = 1700mm, thickness = 30mm.
- Baffle:- $t = 25$,width = 450mm, angle= 7.5° , no = 9, pitch=70mm, tubing=4.
- Cryopanel:- Width = 200mm, $t = 10$ mm, Length = 1000mm, no = 16.
- Dome:- Radius = 720mm, Length = 2500mm.

Thermal Boundary Condition for Tubing Multipanel Cryopump

Sr No	Component name	Temperature	Thermal Accommodation Coefficient
1	Source	300°K	0
2	Dome	300°K	0
3	Radiation shield	80°K	0.1
4	Baffle	80°K	0.1
5	Cryopanel	4.5°K	0.1

Table 5.11: Movak 3D Boundary Condition for Tubing Multipanel Cryopump

Movak 3D Modeling Surfaces for Tubing Multipanel Cryopump

Sr No	Component Name	No of Used
1	circle	1
2	cylinder	5
3	ring	7
4	cone	209
5	parallelogram	144

Table 5.12: Movak 3D Surface Utilization for Tubing Multipanel Cryopump

Movak Modeling Algorithm for Tubing Multipanel Cryopump

- Create circle by define absolute point.
- Create cylinder for dome using relative point.
- Create radiation shield.
- Creation of baffle(use 3D combine transformation for generating tubing).
- Creation of valve.
- Creation of cryopanel.
- Run for 10,00,000 particle.
- Get Transmission Probabiliy and good amount of 80°K particle for it.

Movak Model for Tubing Multipanel Cryopump

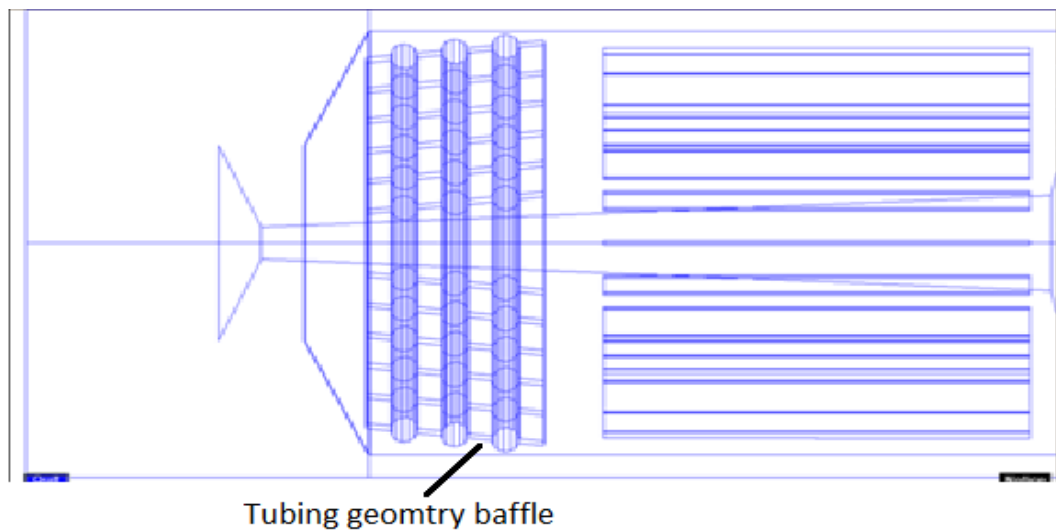


Figure 5.15: Initial Tubing Multipanel Cryopump Movak 3D Modeling

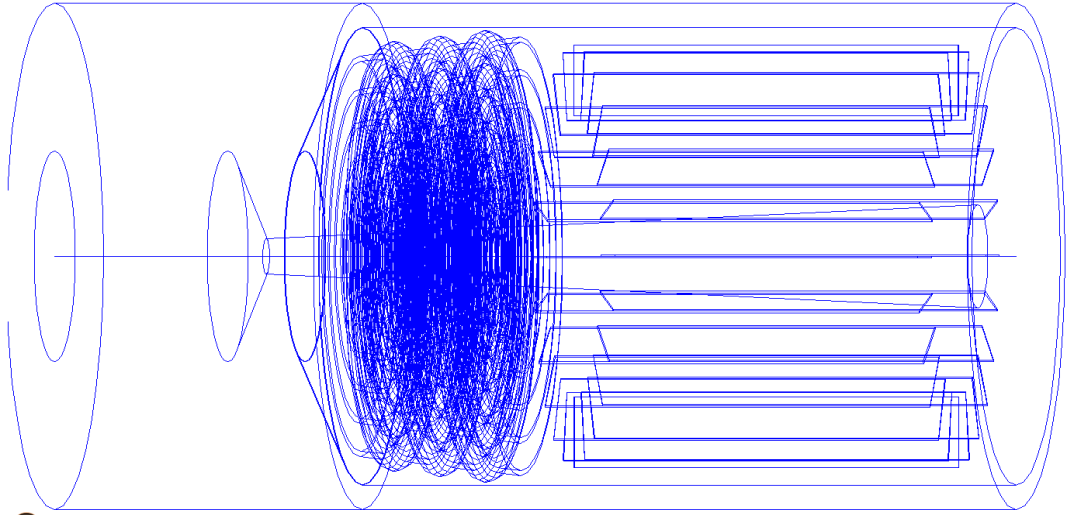


Figure 5.16: 3D View Tubing Multipanel Cryopump Movak 3D Modeling

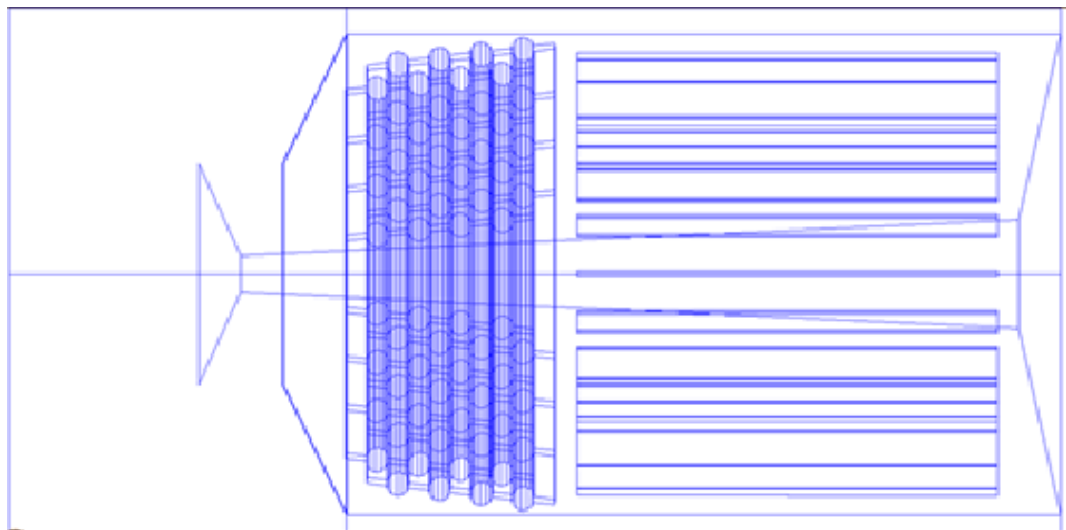


Figure 5.17: Tubing Multipanel Cryopump Modification 1 Movak 3D Modeling

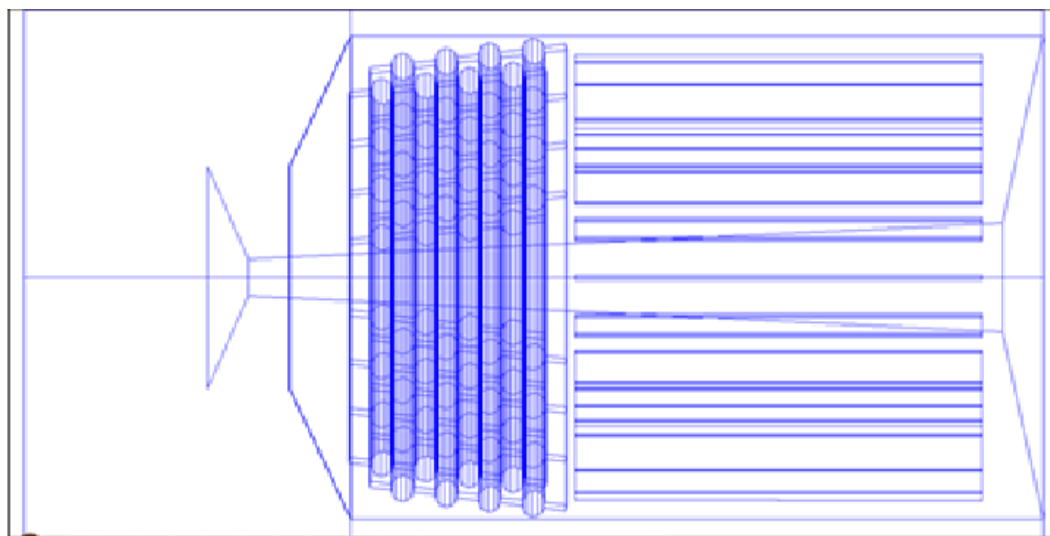


Figure 5.18: Tubing Multipanel Cryopump Modification 2 Movak 3D Modeling

Simulation Result

Table 5.13: Movak 3D Result For 0.1 Thermal Accomodation and 80°K - 90°K Particle

sr no	name	TP	80°K - 90°K particle
1	Initial tubing multipanel cryopump	19.102%	92%
2	Tubing multipanel cryopump modification 1	18.002%	96.5%
3	Tubing multipanel cryopump modification 2	15.181%	98.33%

5.3.6 Pumping Speed Calculation

$$S = c.S_{eff} = c.A_{inlet} \cdot \sqrt{\frac{R_0.T}{2.\Pi.M}} \quad (5.5)$$

$$\frac{1}{c} = \frac{1}{\alpha} + \frac{1}{\omega} - 1 \quad (5.6)$$

Pumping speed for cryopump:- We assume that

- Sticking co efficient =1(for normal gases)

– But actual case

* For hydrogen=0.6

* For helium =0.3

where S=pumpig speed c= capture co-efficnet.

S_{eff} = effective pumping speed.

T.P=transmission Probability.

α = sticking co efficient.

R= gas constant.

T= temperature.

M=molecular mass.

Pumping Speed Calculation for Tubing Multipanel Cryopump

Table 5.14: Pumping Speed for Tubing Multipanel Cryopump

Sr No	name	T.P	Inlet area	Pumping Speed for helium ($\alpha = 0.3$)
1	Initial	19.102%	$0.282857m^2$	$16.65m^3/sec$
2	Modification 1	18.002%	$0.282857m^2$	$15.97m^3/sec$
3	Modification 2	15.181%	$0.282857m^2$	$14.13m^3/sec$

Programming Templet for Various Geometry

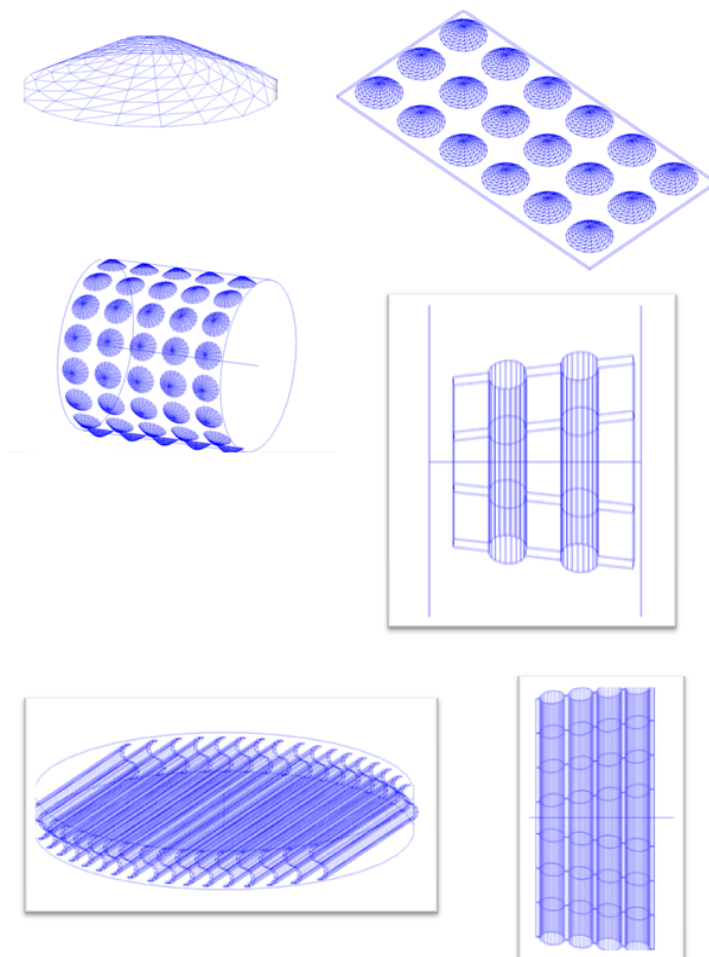


Figure 5.19: Templet for Various Geometry

Chapter 6

Radiation Analysis

6.1 Radiation

Radiation heat transfer is concerned with the exchange of thermal radiation energy between two or more bodies. No medium need exist between the two bodies for heat transfer to take place.

6.1.1 Gray Body Radiation Heat Transfer

Bodies that emit less thermal radiation than a black body have surface emissivity less than 1.

The net heat transfer from a small gray body at absolute temperature T with surface emissivity to a much larger enclosing gray (or black) body at absolute temperatures T_e is given by,

$$\dot{Q} = \epsilon.A.\sigma(T^4 - T_e^4) \quad (6.1)$$

For the case where two objects can see more than just each other, then one must introduce a view factor F and the heat transfer calculations become significantly more involved. The view factor F_{12} is used to parameterize the fraction of thermal power

leaving object 1 and reaching object 2. Specifically, this quantity is equal to,

$$\dot{Q}_{1-2} = A_1 \cdot F_{12} \cdot \varepsilon_1 \cdot T_1^4 \quad (6.2)$$

The case of two black bodies in thermal equilibrium can be used to derive the following reciprocity relationship for view factors.[25]

6.1.2 Theory for Monte Carlo Ray Trace Method

In this method a matrix called radiation exchange factor R is calculated. The difference to the view factor only is that the reflections in all components are included. They shall not be considered as black absorbers and the reflection coefficient of the surface is taken as $1-\varepsilon$, as the view factor matrix equation does. R_{ij} is defined as the portion of the heat flux emitted from the source component i and then absorbed by the target component j. Summing up, the total thermal radiation heat flux absorbed by the target component j is

$$\dot{Q}_j = \sum_{i=1}^n \varepsilon_i A_i \sigma \cdot T_i^4 \cdot R_{ij} \quad (6.3)$$

Exchanging i and j, the net heat flow to the surface i reads:

$$\dot{Q}_{i(net)} = -\varepsilon_i \cdot A_i \cdot \sigma \cdot T_i^4 + \sum_{j=1}^n \varepsilon_j A_j \sigma \cdot T_j^4 \cdot R_{ji} \quad (6.4)$$

The advantage of the MCRT approach is that limitation from the condition to the view factor matrix approach can be removed. The cost is the longer computation time and if the emissivity have been changed, one should redo the Monte Carlo simulation. In Movak 3D radiation heat load is calculated by Monte carlo ray tracing method.[19]

6.2 Radiation Bench Marking

6.2.1 Problem 1

The model shown in below fig includes only five components. They are circle planes P1 and P2 with a diameter of 1.546 m, circle planes P3 and P4 with a diameter of 0.773 m, and a cylinder R1 with a diameter of 1.546 m and a length of 1.784 m. The planes P3 and P4 are two-sided and located at the center of the cylinder R1, with a distance of 35.68mm between them. Two different cases are calculated. And compare with standard literature data result.[19]

case 1 The temperatures of the five components are $T = 300^{\circ}K, 300^{\circ}K, 4.5^{\circ}K, 4.5^{\circ}K, 300^{\circ}K$, and the emissivity are $\varepsilon = 0.9, 0.9, 0.9, 0.9, 0.9$.

case 2 The temperatures keep unchanged, but the emissivity are $\varepsilon = 0.9, 0.9, 0.1, 0.1, 0.9$.

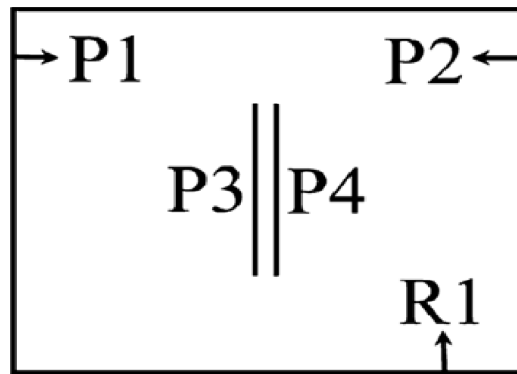


Figure 6.1: Iter Preproduction Cryopump Bench Marking Problem of Paper Monte Carlo Model

Modeling Assignment in Movak 3D

P1=circle 1, P2=ring 1, R1=cylinder 1, P3L=ring 3, P3R=ring 2, P4L=ring 4, P4R=ring 5, Cylinder 2 is connecting of P3Land P3R and cylinder 3 is connecting

P4L and P4R

Simulation Steps for Movak 3D for Radiation Analysis

- Modeling Geometry of given component.(orientation must be correct)
- Assigning Emissivity of surface.(edit in Movak 3d by reflection co efficient=(1-emissivity))
- Switch on radiation heat radiation Heat transfer.
- Assign length scale factor of model.
- Then simulation for 10,00,000 particle.
- Get result in term of radiation heat load.

Simulation Model

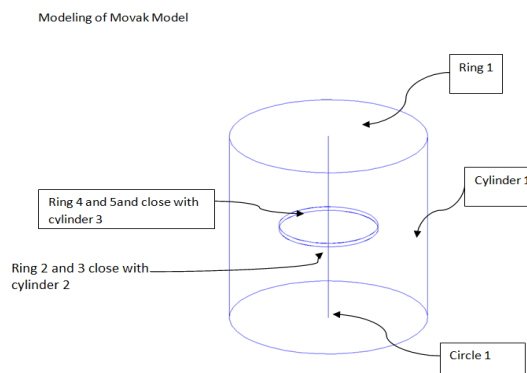


Figure 6.2: Simulation Model in Movak 3D

Simulation Result

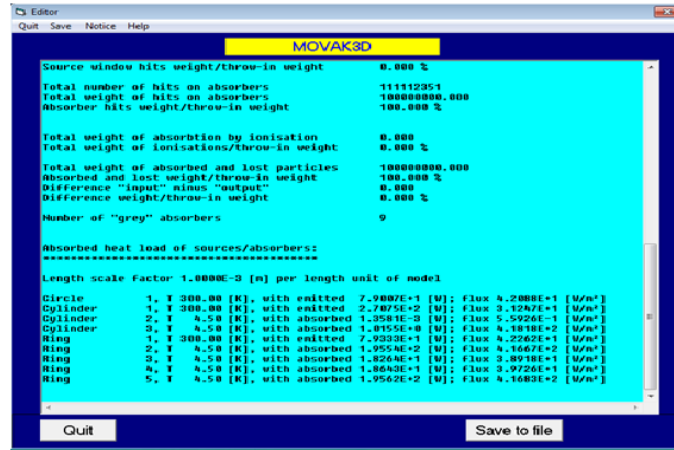


Figure 6.3: Simulation Result for Case 1

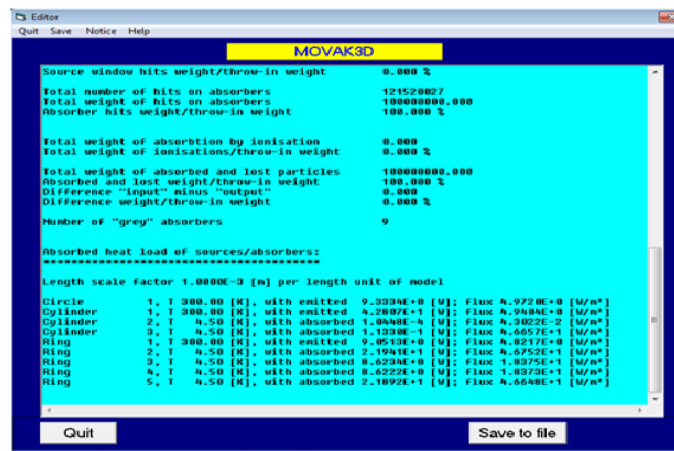


Figure 6.4: Simulation Result for Case 2

Comparison with Literature Data

heat load	binary formula		view factor method		Provac Heat load		Movak Heat load	
P1	-84.82	-19.57	-78.02	-9.36	-78.02	-9.18	-79.00	-9.33
P2	-84.81	-19.57	-78.05	-9.36	-77.56	-9.06	-79.33	-9.05
P3 RIGHT	18.78	11.09	18.66	10.58	18.38	8.51	18.26	8.62
P3 LEFT	202.57	38.95	192.34	21.53	192.2	21.53	195.54	21.94
P4RIGHT	202.67	38.95	192.34	21.53	192.21	21.56	195.62	21.892
P4 LEFT	18.83	11.1	18.68	10.58	18.37	8.51	18.643	8.6222
R1	-273.16	-60.95	-266.01	-45.49	-265.58	-41.87	-270.75	-42.807

Table 6.1: Comparison with Movak 3D Heat Load Data with Standard Literature Data in Terms of Watt

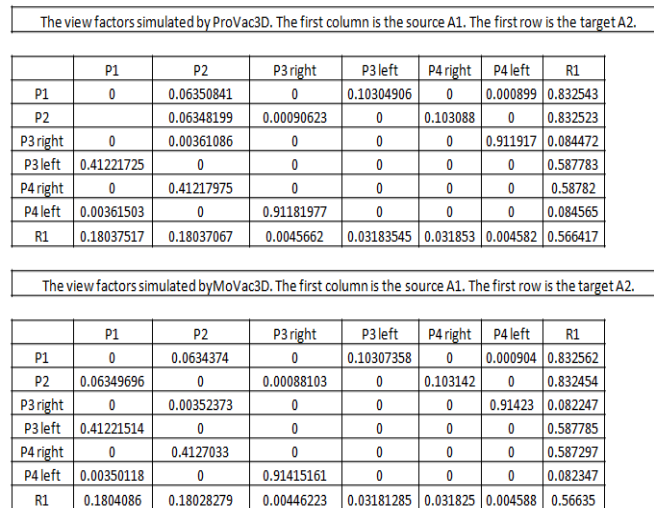


Figure 6.5: Comparison of Movak 3D View Factor Result with Paper Result

Summary

Simulation result and standard literature result data is very nearer.

6.2.2 Verification of Radiation Heat Load by Various Approach for Cylinder Case

Find radiation heat load of given cylinder with the various approach and compare Movak 3D result for it Given data:-

- Cylinder length=500mm
- Cylinder radius=100mm

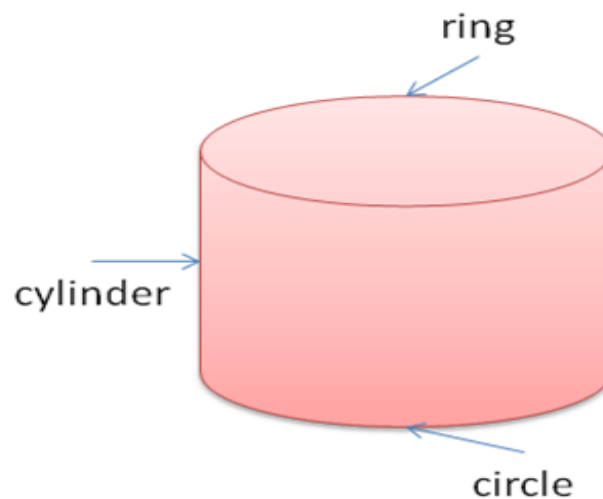


Figure 6.6: Bench Mark Case Model

Boundary condition

Radiation Heat Load by View Factor Approach

View Factor Calculation

Basic Equation for Radiation Heat Transfer

$$Q_{12} = (F_g)_{12} A_1 \sigma_b (T_1^4 - T_2^4) \quad (6.5)$$

Table 6.2: Temperature and Emissivity Data for Cylinder Geometry Bench Marking Case

sr	component	temp	emissivity
1	circle	300°K	0.2
2	cylinder	250°K	0.5
3	ring	200°K	0.4

Table 6.3: View Factor for Cylinder Surface

No	circle	cylinder	ring
circle	0	0.963049	0.036951
cylinder	0.96256	0.807166	0.096578
ring	0.037223	0.962777	0

where

$$(F_g)_{12} = \frac{1}{\left(\frac{1}{\varepsilon_1} - 1\right) + \left(\frac{1}{F_{12}}\right) + \left(\frac{1}{\varepsilon_2} - 1\right)\frac{A_1}{A_2}} \quad (6.6)$$

where

A_1 =source area

A_2 =target area

T_1 =source temperature

T_2 =target temperature

ε_1 =emissivity of source

ε_2 =emissivity of target

F_{12} =view factor 1 to 2

Q_{1-2} =heat transfer from 1 to 2

Heat Load on Various Surfaces

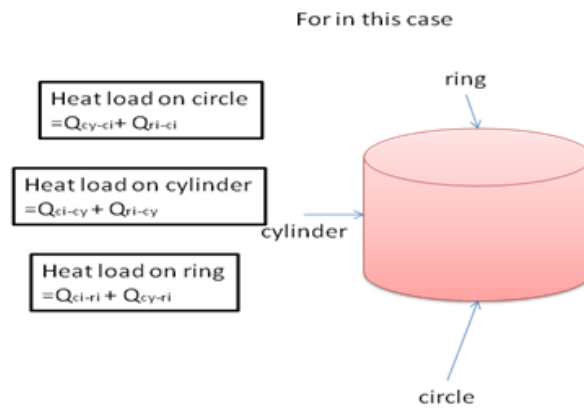


Figure 6.7: Heat Load Bench Mark Case 2

Resultant heat load on various surface

Table 6.4: Heat Load Distribution on Cylinder Surface

Sr No	surface	Temperature	circle	cylinder	ring	total heat load
1	circle	300°K	0W	-1.45631W	-0.35839W	-1.8147W
2	cylinder	250°K	1.456456W	0W	-1.155971W	-0.10325W
3	ring	200°K	0.356214W	1.561616W	0W	1.917831W

(-)Negative sign indicate energy is emitted. (+)Positive sign indicate energy is receiving.

Monte Carlo Ray Tracing Method

In Monte Carlo ray tracing method particle distributed according its energy bundle power

Table 6.5: Probable Movak 3D Particle Distribution for MCRT Approach

sr no	emissivity	temperature	emission power	parti distribution	probable distri
circle	0.2	$300^{\circ}K$	2.937754286	0.074341766	74341.765
cylinder	0.5	$250^{\circ}K$	35.41852679	0.896288648	896288.64
ring	0.4	$200^{\circ}K$	1.160594286 0.	029369586	29369.58

Table 6.6: Particle Distribution in Movak 3D for 10,00,000

Sr	Surface	Particle of Movak simulation=10,00,000
1	Circle	74327
2	Cylinder	896311
3	Ring	29361

Particle Distribution in Movak 3D

Heat Exchanger Factor

R_{ij} is defined as the portion of the heat flux emitted from the source component i and then absorbed by the target component j . Exchanger factor is weighted of surface in simulation and division by emitted particle .[19]

Table 6.7: Heat Exchanger Factor for Pipe Case

	ci	cy	ri
ci	0.037954	0.931509	0.030537
cy	0.037316	0.889911	0.072773
ri	0.015335	0.910836	0.07383

sur-sur	p	sur-sur	p	sur-sur	p	sur-sur	p	total power
ci	-2.93775	ci to ci	0.109625	cy to ci	1.321674	ri to ci	0.017797	-1.488
cy	-35.4185	cy o cy	31.51933	ci to cy	2.736544	ri to cy	1.057111	-0.105
ri	-1.16059	ri to ri	0.085686	cy to ri	2.577519	ci to ri	0.089711	1.592

Table 6.8: Heat Load Distribution in Terms of Watt By MCRT Approach

```

Total weight of absorbed and lost particles      10000000.000
Absorbed and lost weight/throw-in weight      100.000 %
Difference "input" minus "output"             0.000
Difference weight/throw-in weight             0.000 %

Number of "grey" absorbers                    3

Absorbed heat load of sources/absorbers:
*****

Length scale factor 1.0000E-3 [m] per length unit of model

Circle    1, T 300.00 [K], with emitted 1.4867E+0 [W]; flux 4.7324E+1 [W/m²]
Cylinder  1, T 250.00 [K], with emitted 1.1391E-1 [W]; flux 3.6260E-1 [W/m²]
Ring      1, T 200.00 [K], with absorbed 1.6006E+0 [W]; flux 5.0950E+1 [W/m²]
    
```

Figure 6.8: MOVAK 3D HEAT LOAD

SR	Surface	Theoretical	MCRT approach	Movak 3d result
1	Circle	-1.8147W	-1.48866W	-1.4867W
2	Cylinder	-0.10325W	-0.10554W	-0.11391W
3	ring	1.917831W	1.592322W	1.6006W

Table 6.9: Comparison of Various Approach for Heat Load Data

Summary

Radiation heat load data is very nearer to various approach.

6.2.3 Radiation Analysis Bench Mark with Ansys

Radiation analysis of cylindrical geometry. Geometry Data :- Radius = 25mm

Length = 100mm

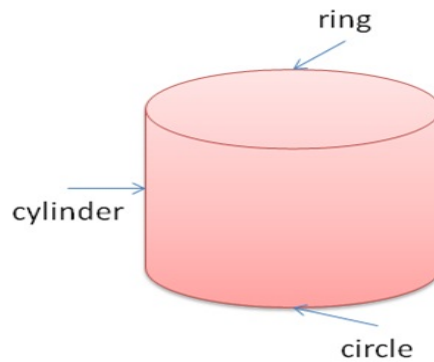


Figure 6.9: Geometry for Ansys Bench Marking

Table 6.10: Boundary Condition for Ansys View Factor Case for Radiation Heat Load Study

Sr	component	Temp	Emissivity
1	circle	$700^{\circ}K$	0.8
2	cylinder	$800^{\circ}K$	0.75
3	ring	$700^{\circ}K$	0.8

Resultant heat load on cylinder to circle=In cylinder geometry view factor for radiation from cylinder to circle $F_{23}= 0.01558$ (from ansys).

Shape factor $F_{21} = 1 - F_{23}$ (circle to cylinder).

The theory of reciprocity $A_1.F_{12} = A_2.F_{21}$.

So heat load from circle to cylinder is $Q_{12}=(F_g)_{12}A_1\sigma_b(T_1^4 - T_2^4)=3.66\text{Watt}$.

Movak 3D Result

```

Editor
File Save Notice Help

MOVAK3D

Circle 1 with 75077837 hits: weight 60060160.000
Cylinder 1 with 1173206963 hits: weight 879876300.000
Ring 1 with 75001552 hits: weight 60003540.000

Total number of hits on source windows 0
Total weight of hits on source windows 0.000
Source window hits weight/throw-in weight 0.000 %

Total number of hits on absorbers 1023366352
Total weight of hits on absorbers 1000000000.000
Absorber hits weight/throw-in weight 100.000 %

Total weight of absorption by ionisation 0.000
Total weight of ionisations/throw-in weight 0.000 %

Total weight of absorbed and lost particles 1000000000.000
Absorbed and lost weight/throw-in weight 100.000 %
Difference "input" minus "output" 0.000
Difference weight/throw-in weight 0.000 %

Number of "grey" absorbers 3

Absorbed heat load of sources/absorbers:
*****
Length scale factor 1.0000E-3 [m] per length unit of model

Circle 1, 1 700.00 [K], with absorbed 3.5725E+0 [W]; Flux 7.2778E+3 [W/m^2]
Cylinder 1, 1 800.00 [K], with emitted 7.1449E+0 [W]; Flux 9.8972E+2 [W/m^2]
Ring 1, 1 700.00 [K], with absorbed 3.5724E+0 [W]; Flux 7.2777E+3 [W/m^2]

```

Figure 6.10: Movak 3D Result for Ansys Bench Marking

Summary

Movak 3D calculation is nearer to Ansys view factor approach result.

6.3 Project part :- Radiation Heat Load Analysis For Single Panel Cryopump by Movak 3D

Assembly Name:- Single Panel Cryo Pump.

Subassembly of single panel cryo pump:-

- Cryopanel.
- Louver Baffle.
- Front particle diverter.
- Conical radiation shield.
- Cylindrical radiation shield.
- Rear end shield.
- Dome cover.
- Source pipe.

Dimension of Cryopump

Cryopanel Length = 1000mm, Width = 200mm, Thickness = 10mm.

Radiation shield Inner radius = 430mm, Length = 1200mm, Thickness = 30mm.

Dome radius = 500mm, Length = 2400mm.

Louver Baffle No = 15, Inner radius = 300, Outer radius = 370, Width of baffle = 70mm.

Front Particle Diverter Cone radius = 115mm, Width = 200mm, Thickness = 3mm.

Front cone radiation shield Outer radius = 300mm, Inner radius = 200mm, Length = 150mm.

Table 6.11: Boundary Condition for Single Panel Cryopump

Sr	Compt name	Temp	Thermal Accom Coeff	Emissivity
1	Cryo panel	4.5 °K	0.4	0.9
2	Louver Baffle	80 °K	0.4	0.9
3	Front particle diverter	80 °K	0.4	0.35
4	Conical radiation shield	80 °K	0.4	0.35
5	Cylindrical radiation shield	80 °K	0.4	0.35
6	Rear end shield	80 °K	0.4	0.35
7	Dome cover	300 °K	0.4	0.1
8	Source Pipe	300 °K	0.4	0.1

Table 6.12: Surface Element Include for Single Panel Cryopump

Sr No	Component Name	No
1	parallelogram	6
2	circle	1
3	cylinder	36
4	cone	39
5	ring	8

Movak 3D Modeling Algorithm for Radiation Analysis

- Create Programme for single panel cryopump with mcl language.
- Change reflection co efficient by (1-emissivity).
- Transfer model to radiation heat transfer on.
- Scale model for analysis for conversion mm scale model to meter.
- Run for 10,00,000 particle.
- Radiation heat load data obtain for out put surface in terms of .txt file.

Movak 3D Modeling for Single Panel Cryopump

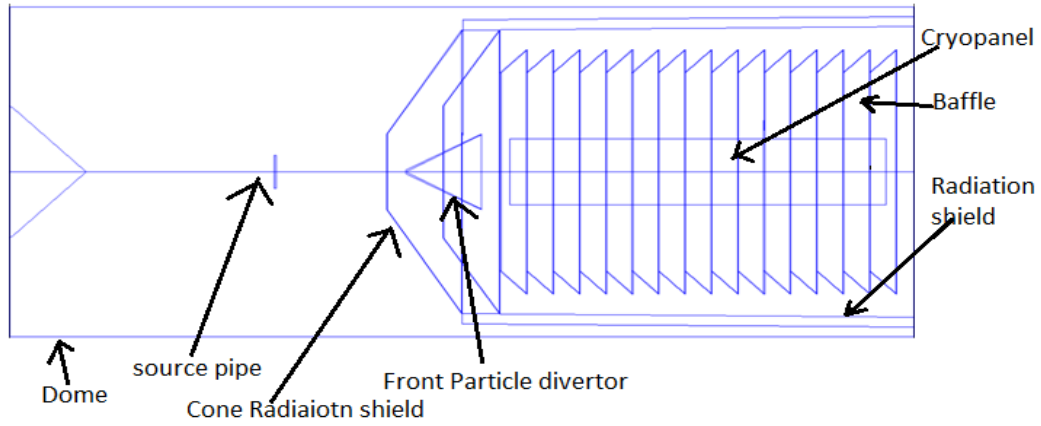


Figure 6.11: Movak 3D Model for Single Panel Cryopump

Movak 3D Radiation Heat Load Result

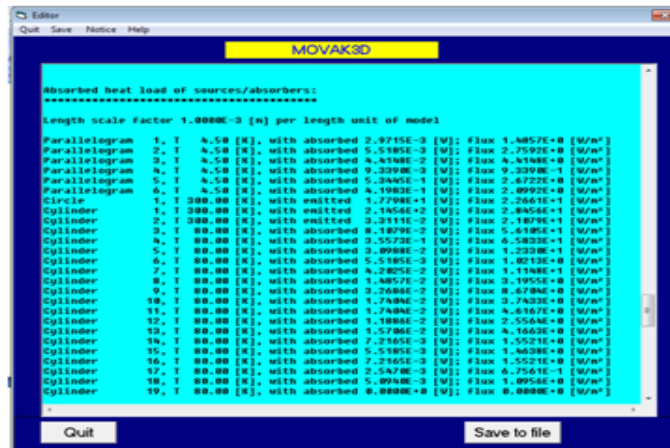


Figure 6.12: Movak 3D Result for Single Panel Cryopump

Visibility for Heat Load Distribution

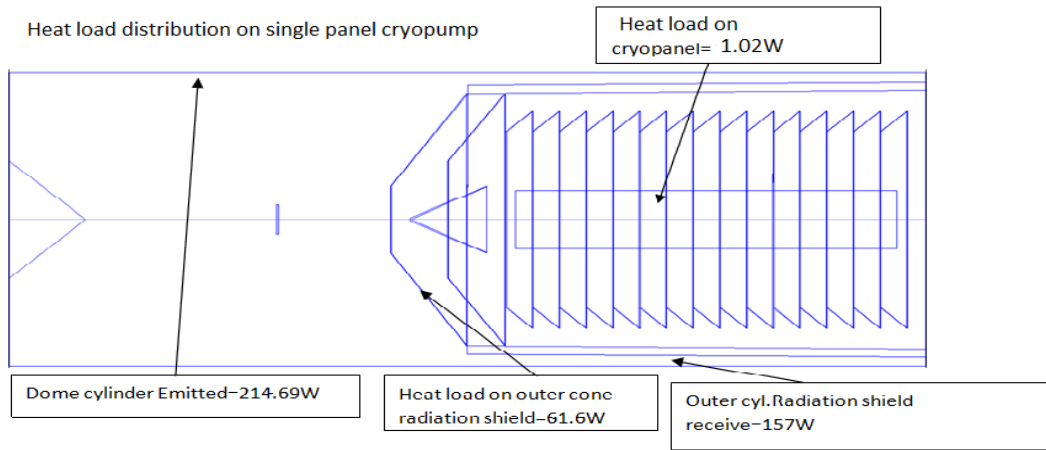


Figure 6.13: Movak 3D Heat Load Distribution for Single Panel Cryopump

Radiation heat Load Data for Single Panel cryopump Major Component

Table 6.13: Heat Load Distribution for Single Panel Cryopump

Sr No	Component name	Heat load in terms of Watt
1	Dome cylinder surface	-214.69W
2	Dome circle surface	-17.61W
3	cylinder Radiation outer shield	157W
4	Cylinder radiation shield inner	2.28W
5	1st Cone radiation shield outer	61.6W
6	1st Cone radiation shield inner	2.17W
7	Particle diverter outer	0.951W
8	Cryo panel	1.02W
9	2nd cone radiation shield outer	1.42W

6.4 Radiation Heat Load Minimization in Single Panel Cryopump

6.4.1 Minimization of Radiation Heat Load on Cryopanel

In single panel cryopump emissivity for outer radiation shield is 0.35 and baffle facing to cryopanel is 0.9. but from literature survey of (basic and application of cryopump). Emissivity of outer radiation shield if we take 0.9 and emissivity of inner baffle facing (last 11 baffle) to cryopanel is 0.1. Then radiation heat load on cryopanel is decrease.

6.4.2 Result of Movak 3D Simulation for Modified Emissivity

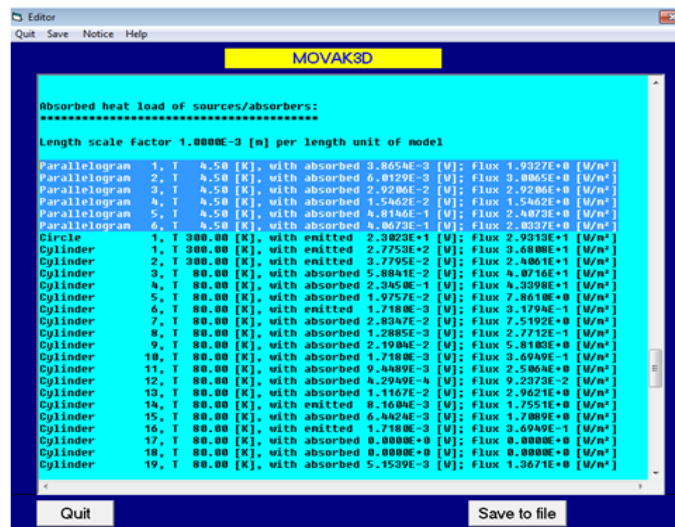


Figure 6.14: Movak 3D Heat Load Distribution for Optimized Emissivity Single Panel Cryopump

Heat Load On Cryopanel

Parallelogram 1, T 4.5 [K], with absorbed 3.87E-03 [W];

Parallelogram 2, T 4.5 [K], with absorbed 6.01E-03 [W];

Parallelogram 3, T 4.5 [K], with absorbed 2.92E-02 [W];

Parallelogram 4, T 4.5 [K], with absorbed 1.55E-02 [W];

Parallelogram 5, T 4.5 [K], with absorbed 4.81E-01 [W];

Parallelogram 6, T 4.5 [K], with absorbed 4.07E-01 [W];

Total 9.43E-01 [W];

Summary

Radiation Heat load on cryopanel is reduce up to 0.94W.

Chapter 7

CFD Analysis For Cryopanel

7.1 Cryopanel Fluid Analysis

Flow distribution through cryopanel much more important for maintaining surface temperature below $5^{\circ}K$. So such type of geometry work as a heat exchanger during pumping and regeneration mode of cryopump. For Temperature Profile is depend on flow distribution of fluid in cryopanel. For that case flow distribution must be study for cryopumping application. In Ansys Fluent flow analysis of ScHe at temperature below $5^{\circ}K$ will be possible. Here in that case inlet pressure condition is 0.4MPa and outlet pressure condition is 0.35MPa. Heat load acting on cryopanel involve so many factor. but in our case we assume that heat load acting on cryopanel is $25W/m^2$. Inlet Temperature of fluid is 4.2K and outlet temperature of cryopanel system is 4.7K.

7.2 Cryopanel Thermal Fluid Analysis

In cryopanel heat is generated during cryopumping should not exceed the boiling point of ScHe during cryopumping. so Flow rate and Pressure drop should be such that it should not exceed temperature of fluid during cryopumping.

7.3 Bench marking

7.3.1 Pressure Drop in Circular Pipe

Water is passing through the tube, which has diameter of 60mm and length of pipe is 3m. Inlet velocity of pipe is 5m/sec. Assume friction less condition. Wall has velocity is equal to zero. Consider water is incompressible.

Property of Water

Table 7.1: Water Property for 20 C

Density (kg/m ³)	993.95
Viscosity (Pa Sec)	7.282x10 ⁻⁴
Specific Heat (J/Kg K)	4174
Conductivity (W/m K)	0.6253

Theoretical Calculation

Reynold's Number

$$Re = \frac{\rho \cdot V \cdot D}{\mu} \quad (7.1)$$

$$= \frac{993.95 \times 3 \times 0.06}{7.282 \times 10^{-4}} \quad (7.2)$$

$$= 409201.3 \quad (7.3)$$

Hence, Flow is turbulent

Friction Factor

$$f = \frac{0.0791}{Re^{\frac{1}{4}}} \quad (7.4)$$

$$= \frac{0.0791}{409201.3^{\frac{1}{4}}} \quad (7.5)$$

$$= 3.127 \times 10^{-3} \quad (7.6)$$

Head loss due to friction

$$h_f = \frac{4.f.l.v^2}{2.g.d} = \frac{4 \times 3.127 \times 10^{-3} \times 3 \times 5^2}{2 \times 9.81 \times 0.06} = 0.796m \quad (7.7)$$

Pressure drop due to friction:-

$$\Delta.P.h.f = 0.796 \times 993.95 \times 9.81 = 7761.52Pa \quad (7.8)$$

Pressure drop drive from Moody chart :- friction factor=0.135 Pressure Drop =8386Pa

7.3.2 Simulation of Pressure Drop in Ansys Fluent

Pipe Modeling

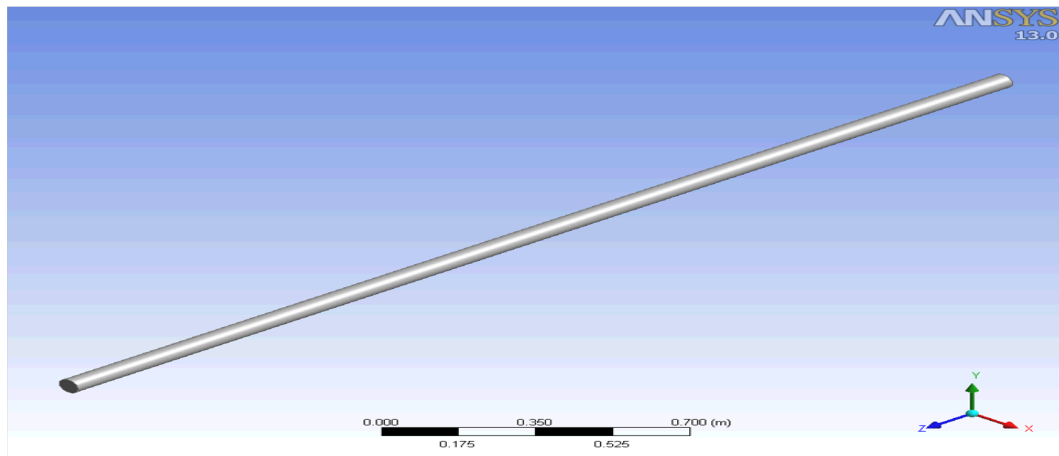


Figure 7.1: Modeling of Pipe

Meshing

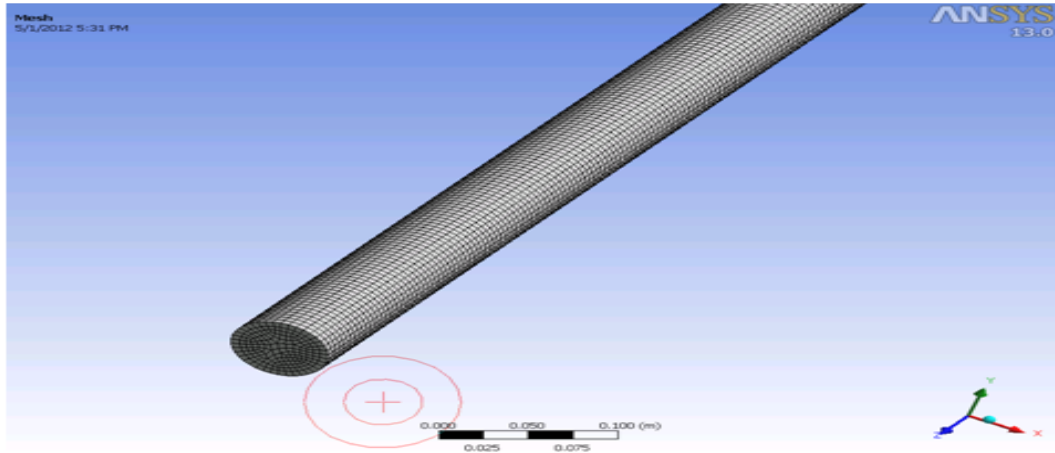


Figure 7.2: Meshing of Pipe

Pressure Drop

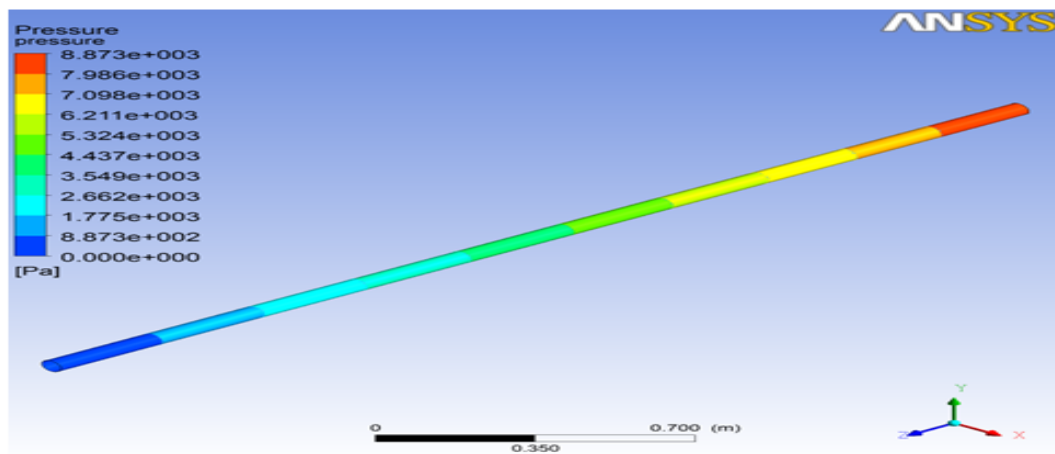


Figure 7.3: Pressure Drop in Pipe

Summary

Simulation result and theoretical result are nearly same.

7.3.3 Nozzle Velocity

Water is passing through the nozzle. $d_1 = 0.1$ m, $d_2 = 0.05$ m, Length of the nozzle = 0.2 m, Inlet Velocity = 1.5 m/s

Property of Water

Table 7.2: Water Property

Density (kg/m ³)	993.95
Viscosity (Pa Sec)	7.282x10 ⁻⁴
Specific Heat (J/Kg K)	4174
Conductivity (W/m K)	0.6253

Theoretical calculation:- $A_1V_1 = A_2V_2$

where $A = \frac{\pi}{4}D^2$ $D_1=0.1$ m $D_2=0.05$ m $V_1 = 1.5$ m/s

final outlet velocity $V_2=6$ m/s

bernoulli equation for pipe flow is:-

$$\frac{P_1}{\rho \cdot g} + Z_1 + \frac{V_1^2}{2 \cdot g} = \frac{P_2}{\rho \cdot g} + Z_2 + \frac{V_2^2}{2 \cdot g} \quad (7.9)$$

$$P_1 - P_2 = \left(\frac{V_2^2 - V_1^2}{2} \right) \rho \quad (7.10)$$

$$P_1 - P_2 = 16772.9 \text{ Pa} \quad (7.11)$$

7.3.4 Analysis of Nozzle

Meshing

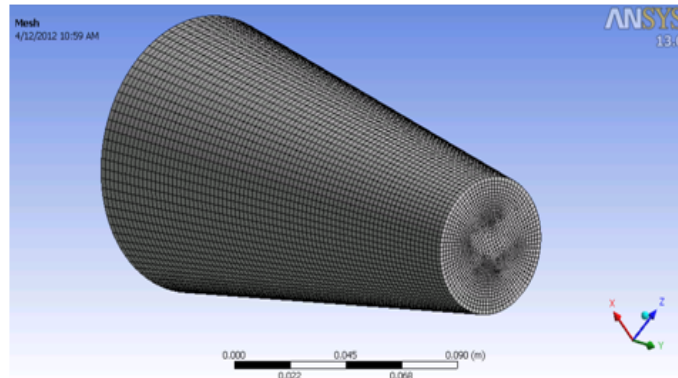


Figure 7.4: Meshing of Nozzle

Pressure drop in nozzle

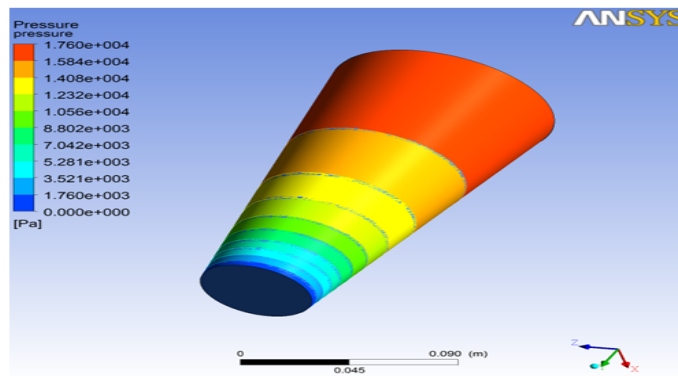


Figure 7.5: Pressure Drop in Nozzle

Velocity vector in nozzle

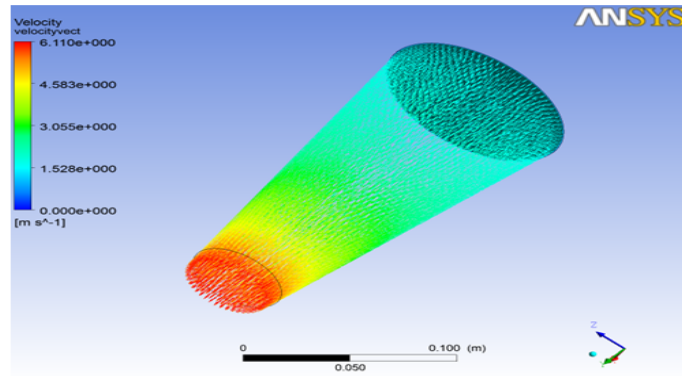


Figure 7.6: Velocity in Nozzle

Summary

simulation result and theoretical result are same for case of nozzle.

7.4 Project Part Analysis

7.4.1 Seam Welded cryopanel

Dimension of Cryopanel

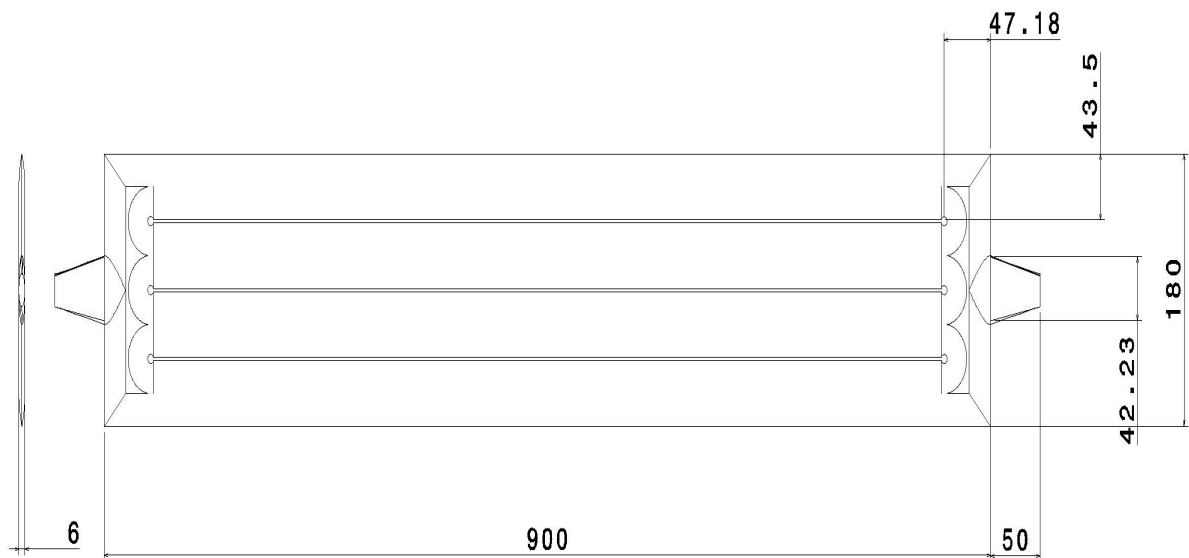


Figure 7.7: Seam Welded Cryopanel Dimension

Boundary Condition

- Inlet Pressure=0.4MPa
- Outlet Pressure=0.35MPa
- Wall Heat Flux= $25W/m^2$
- Wall Velocity =0
- Mass Inlet Fluid Temperature=4.2K

Table 7.3: Liquid Helium Property at 4.2K

Density (kg/m ³)	138.3
Viscosity (Pa Sec)	3.87x10 ⁻⁶
Specific Heat (J/Kg K)	3556
Conductivity (W/m K)	21.7x10 ⁻³

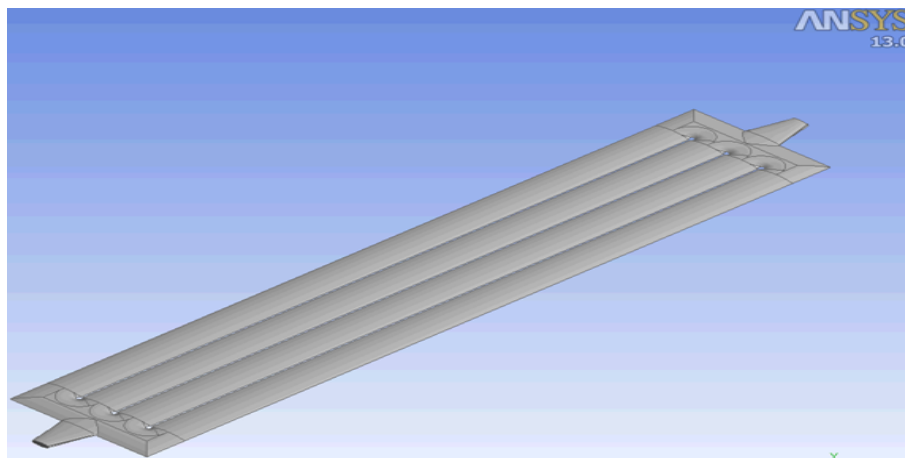


Figure 7.8: Seam Welded Cryopanel

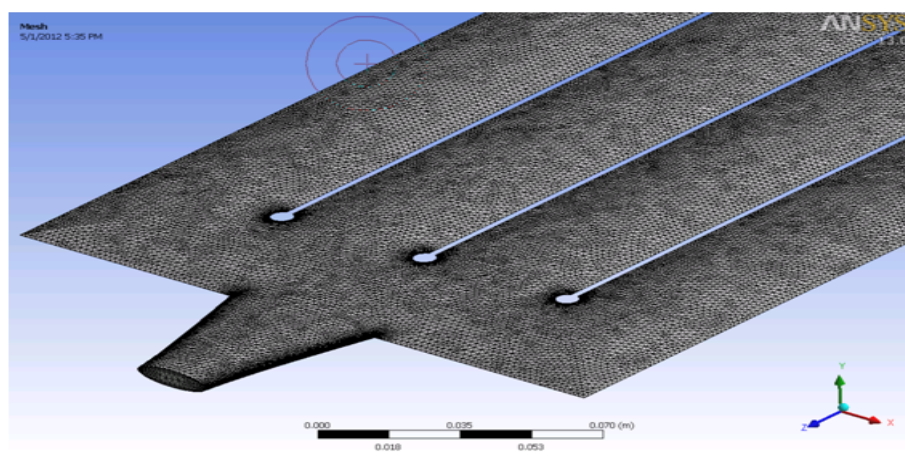


Figure 7.9: Meshing of Seam Welded Cryopanel

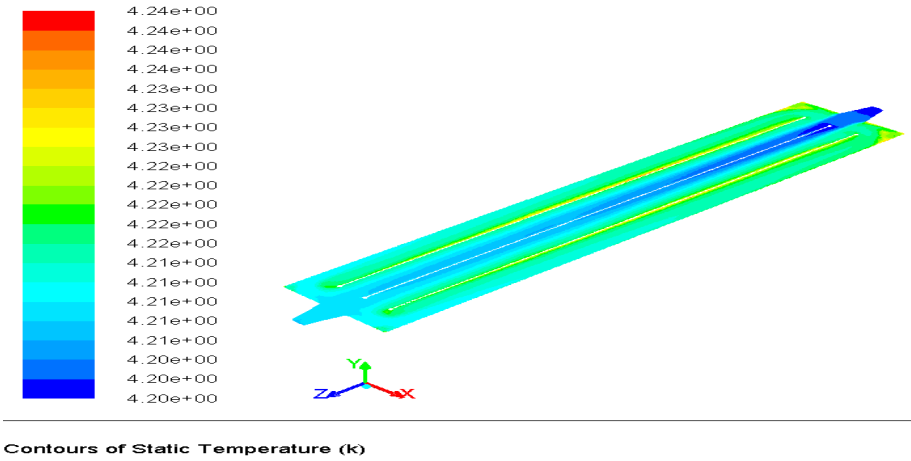


Figure 7.10: Temperature Profile of Seam Welded Cryopanel

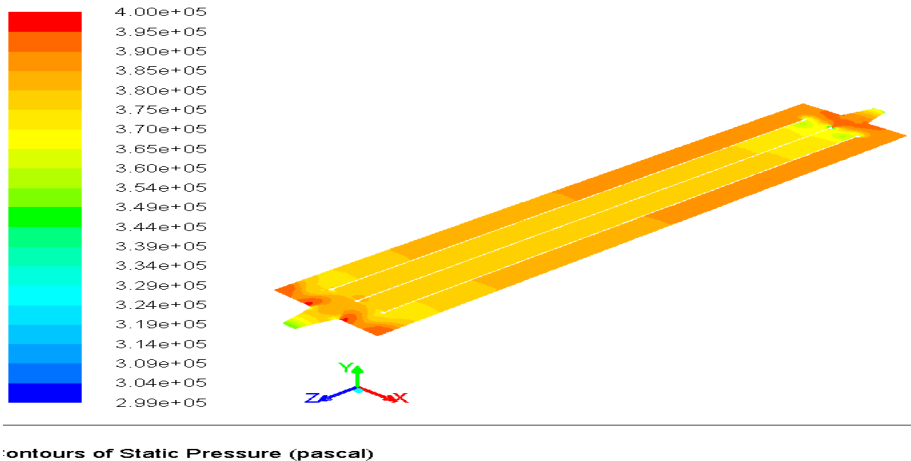


Figure 7.11: Pressure Profile of Seam Welded Cryopanel

7.4.2 Bubble Form Cryopanel

Dimension of Cryopanel

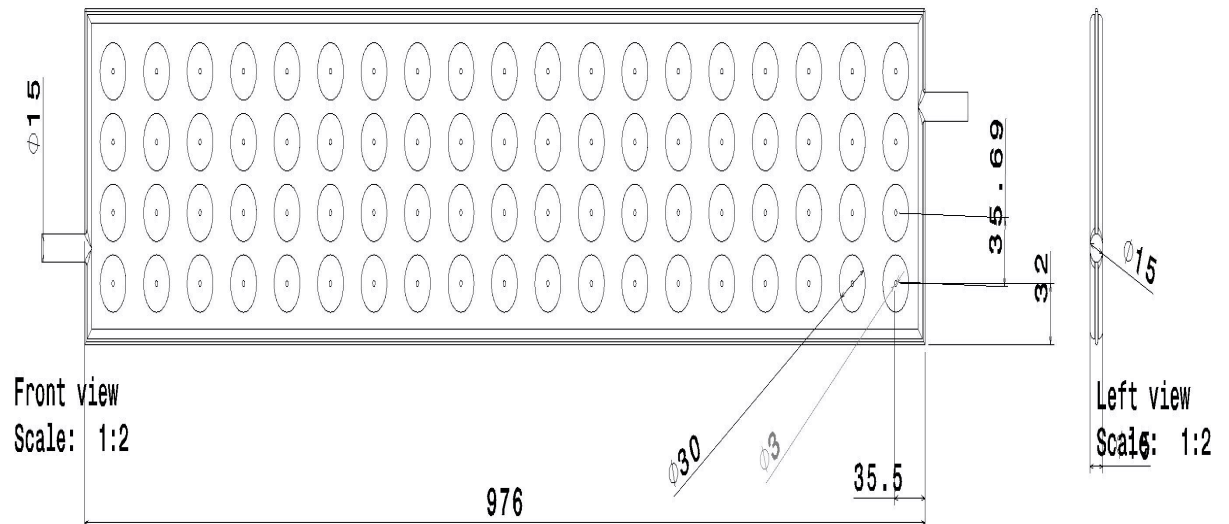


Figure 7.12: Bubble Cryopanel Dimension

Boundary Condition for Bubble cryopanel

- Inlet pressure=0.4 MPa
- Outlet pressure=0.35 MPa
- Wall heat flux= $25W/m^2$
- Wall velocity =0
- Inlet fluid Temperature=4.2K

Table 7.4: Property for Liquid Helium at 4.2K

Density (kg/m ³)	138.3
Viscosity (Pa Sec)	3.87x10 ⁻⁶
Specific Heat (J/Kg K)	3556
Conductivity (W/m K)	21.7x10 ⁻³

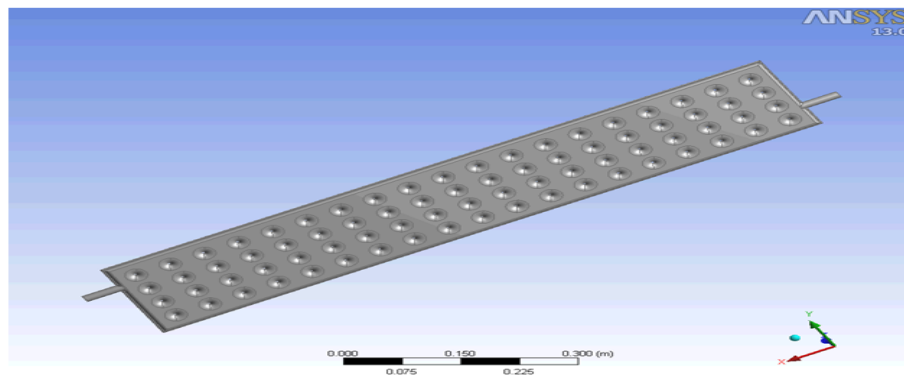


Figure 7.13: Bubble Cryopanel Dimension

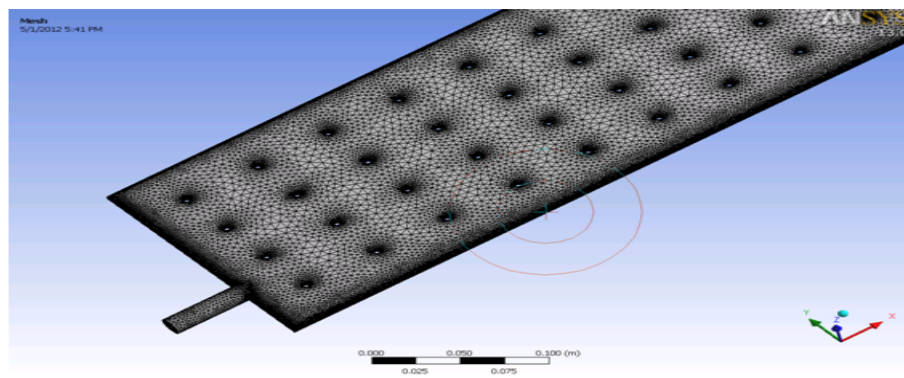


Figure 7.14: Meshing of Bubble Cryopanel

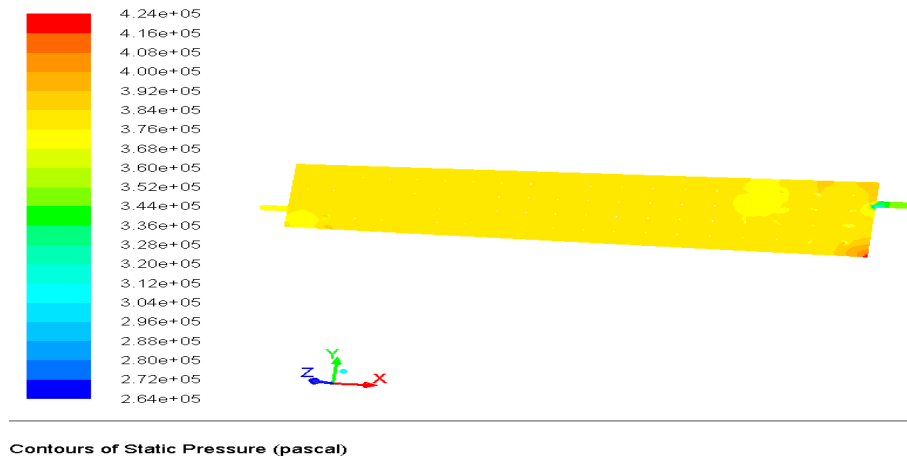


Figure 7.15: Pressure Profile of Bubble Cryopanel

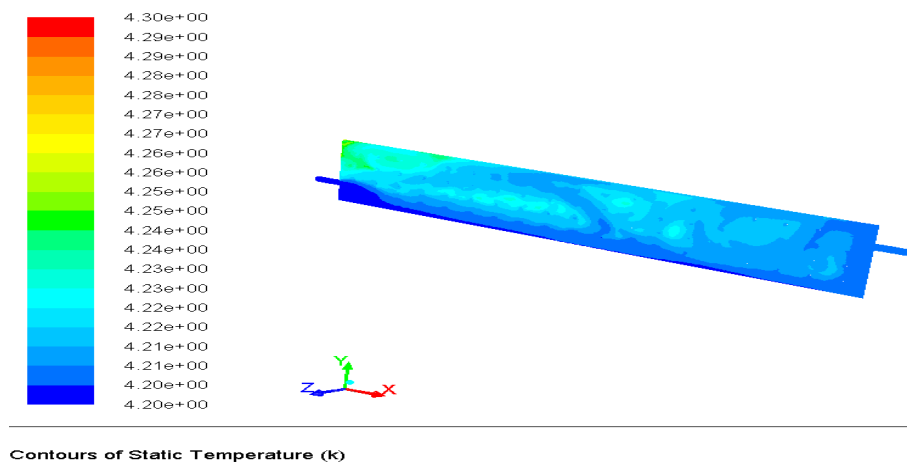
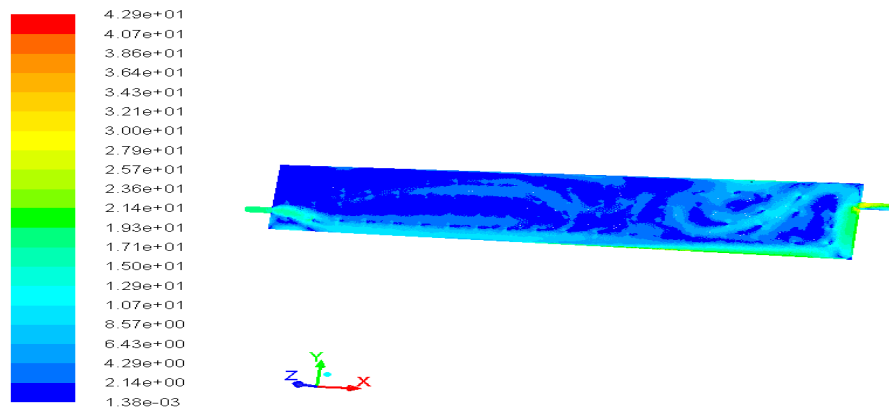


Figure 7.16: Temperature Profile of Bubble Cryopanel



Velocity Vectors Colored By Velocity Magnitude (m/s)

Figure 7.17: Velocity vector Profile of Bubble Cryopanel

Chapter 8

Results

8.1 Molecular Flow Analysis

- In Molecular Flow Analysis angle of twist for helix at 60° at particular L/D ratio is optimized geometry for maximum molecular gas temperature reduction and maximum transmission probability.
- Tubing Geometry of multipanel cryopump produced 98% 80-90⁰K particle under 0.1 accommodation co efficient of 80⁰K temperature surfaces. So such geometry is efficient geometry for maximum transmission probability and more number of 80-90⁰K temperature gas particle Temperature.

8.2 Radiation Analysis

- In single panel cryopump radiation heat load generated by 300 ⁰K temperature surface is mainly absorbed by radiation shield outer wall and conical radiation shield of cryopump.
- In single panel cryopump from 15 baffle out of 3 baffle absorb radiation heat load from the 300⁰K and rare 12 baffle emitted radiation heat load on cryopanel.in that case radiation heat load acting on cryopanel is approximately 1.02W.

- In radiation analysis of cryopump, emissivity is of louver baffle of last 10 baffle should be minimize for radiation heat load reduction. In that case radiation heat load decrease from 1.02W to 0.94W.

8.3 CFD Analysis

- Flow distribution in case of seam welded cryopanel is not uniform. for that case inlet channel should be modified for uniform fluid flow. In this simulation case temperature is not rising beyond 4.5⁰K. In seam welded cryopanel due to stagnation of fluid to wall body little pressure is built up in that case.
- flow distribution is not uniform for bubble panel . In this simulation case temperature is not rising beyond 4.5⁰K.

Chapter 9

Conclusion and Future Scope

Molecular Flow Analysis

- Specially design Cryopump is required for pumping out exhaust gases during fusion process in fusion reactor, as very high pumping system is needed. Traditional industrial cryopump is not convenient suitable for fusion reactor and cryopump is modified according to tokamak situation.
- The cryopump requires design considering max transmission probability, minimum heat load and optimum temperature of gas particle striking on cryopanel. This require optimization of cryopump geometry. For More saturation limit of gases cryosorption multi panel cryopump is good for efficient pumping.
- So from no of modification of geometry of cryopump and simulation result, fusion reactor exhaust gases produce will be pumped by tubing multipanel cryopump efficiently.

Radiation Analysis

- In Radiation Analysis in case of complicated geometry is very difficult. MCRT method approach is one of the good approach for Radiation heat load estimation for cryopump.

CFD Analysis

- Cryopanel needed uniform for heat transfer of cryopanel surfaces. For that case flow distribution should be uniform. So inlet section should be modified. In case of bubble panel inlet portion entry should be offset to center and seam welded panel is should uniformly varying cross section area. CFD analysis will be used to optimize inlet section entry and uniform flow distribution.

9.1 Future Scope

Molecular Flow Analysis

- DSMC simulation of cryopump.
- Molecular flow analysis of diverter for cryopump.
- Experimental study of thermal accommodation for Hydrogen and Helium at cryogenic temperature.

Radiation Analysis of Cryopump

- Experimental study for radiation heat load.
- Radiation analysis by Provac3D for molecular and radiation combine heat load analysis.
- Radiation analysis of coating material of radiation shield.

CFD Analysis

- Study for inlet geometry for minimum pressure drop and uniformly flow distribution.
- Experimental study of pressure drop for cryopump component.

Appendix A

Property

Table A.1: Liquid helium property at lower temperature

Temperature	4.2°K	4.4°K	4.6°K	4.8°K	5.0°K	5.2°K	5.4°K	5.6°K
Density(Kg/ m^2)	138.3	135.4	132.1	128.3	123.8	118.3	112.3	104.7
Specific heat(J/Kg-K)	3556	3914	4346	4884	5578	6404	7569	9573
Viscosity (Pa.S)x10-7	38.7	37.5	36.2	34.9	33.5	32.0	30.6	29.0
Conductivity(W/m-K)x10-3	21.7	22.0	22.1	22.2	22.1	22.0	21.9	21.7

References

- [1] C. Day, “Basics and applications of cryopumps”, Forschungszentrum Karlsruhe, Institute of Technical Physics, 76344 Eggenstein-Leopoldshafen, Germany.
- [2] Charles B. Hood, “The development of large cryopumps from space chambers to the fusion program”, Journal of vacuum science and Technology A, 3 (3), May/Jun 1985.
- [3] G. Schafer and H.-U. Hafner, “Cryopumps for evacuating space simulation chambers”, Journal of vacuum science and Technology A, 5 (4), Jul/Aug 1987.
- [4] D. W. Sedgley, T.H. Batzer and W.R. Call, “Helium cryopumping for fusion applications”, Journal of vacuum science and Technology A, 6 (3), May/Jun 1988.
- [5] S. Nesterov and J. Vasiliev, L. C. Wagner and M. Boiarski, “Hydrogen pumping simulation for cryopumps”, Journal of vacuum science and Technology A, 17.4., Jul/Aug 1999.
- [6] Douglas W. SEDGLY and Albert G. Tobin, Thomas H. Batzer and Wayne R. CALL, “Cryopumping for fusion reactors”, Nuclear Engineering and design, fusion 4, north Holland, Amsterdam, 1958, page 149-163.
- [7] A. W. Ross and M. Fink, H. F. Wellenstein, “Monte Carlo simulation of chevron baffle performance”, Journal of vacuum science and Technology A, 11(3), May/Jun 1993.
- [8] Yoshitane Akiyama, Katsuya Nakayama and Mahito Saito, “Calculation of Cryopumping speeds by the Monte Carlo method”, Vacuum, Volume 21, number 5, revised 1, January 1971, Page-167.
- [9] J W Lee and Y K Lee, “Calculation of capture coefficients for a cylindrical cryopump Calculation of capture coefficients for a cylindrical cryopump”, Vacuum, Volume 42, Numbers 8/9, 1991, Pages 555-560.
- [10] S G Gilankar and P K Kush, “Experimental verification of capture coefficients for a cylindrical cryopanel of closed cycle refrigerator cryopump”, Journal of Physics Conference Series 114 (2008) 012058.

- [11] Xu tingwai,Xu Li,Zang shuxiu, “Calculations of pumping coefficients for cryopumps using a combined Oatley-Monte Carlo method”, *Vacuum*, Volume 39,Number 6,Page 543 to 546,1989.
- [12] Chr. Day, A. Schwenk-Ferrero, “Sticking coefficient for helium and helium-containing mixtures at activated carbon under liquid helium cooling conditions”, *Vacuum*,Volume 53,1999,Page 253-256.
- [13] Ozdemir and D. Perinica, “Helium sticking coefficient on cryopanel coated by activated carbon”, Forschungszentrum Karlsruhe, GmbH, Hauptabteilung Ingenieurtechnik,Posfach 3640,D-76021 Karlsruhe,Germany.
- [14] Xueli Luo,Christian Day, Horst Haas, and Stylianos Varoutis, “Experimental results and numerical modeling of a high-performance large-scale cryopump. I. Test particle Monte Carlo simulation”, *Journal of vacuum science and Technology A* 29(4),Jul/Aug 2011,Pages 041601-1.
- [15] X. Luo , Chr. Day, “3D Monte Carlo vacuum modeling of the neutral beam injection system of ITER”, *Fusion Engineering and Design* 85 (2010) 1446-1450.
- [16] J.P Hobson, “Accommodation Pumping -A New Principle for Low Pressures”, *The Journal of Vacuum Science and Technology* ,volume7,no 2,28 july 1969.
- [17] O C Dermoire and P W Schmidt, “A 20 K cryopump with a high conductance baffle design”, *Vacuum*, volume 30,number 10, received 2 July 1980.
- [18] J.P Hobson, “Accomodaion Pumping -A new principle for low Pressure”, *the journal of vacuum science and technology* ,vol 7, no 2,1969.
- [19] Xueli Luo, Volker Hauer, Christian Day, “Monte Carlo calculation of the thermal radiation heat load of the ITER pre-production cryopump”, *Fusion Engineering and Design*, FUSION-615, 2012.
- [20] W Obert and G PeriniC, “Pumping speed and thermal load analysis of the JET appendage cryopump by Monte Carlo calculation”, *Vacuum*, Volume 43,1992, Page163-166.
- [21] R.A .Hafer ,“Cryopumping theory and practice ”, Clarendon Press, Oxford 1989.
- [22] A.Roth,“vacuum technology ”, North-Holland, 1990.
- [23] Kimo M. Welch,“Capture Pumping Technology”,2nd fully revised, North-Holland,2001.
- [24] J. Robert Mahan,“Radiation Heat Transfer: A Statistical Approach” ,John Wiley and sons,2002
- [25] D.S.Kumar,“heat and mass transfer”,S. K. Kataria and Sons, 2009.

- [26] R.K bansal, "fluid mechanics and hydraulic machine", luxmi publication, 2005.
- [27] Gottfried Class, "Movak3D user Manual, Lauterbach Verfahrenstechnik, Germany.
- [28] Wang Juan, Ouyang Zhengrong, Zhu WU, Hu Chundong, "Structural Analysis and Calculation for the Radiation Baffle of Cryopumps", Plasma Science and Technology, vol.1.7, No.4, Aug. 2005.
- [29] Bao Min, Fu Xin, Chen Ying, " Computational Fluid Dynamics Approach to Pressure Loss Analysis of Hydraulic Spool Valve" ,Scholl Frank Technical University of Karlsruhe (TH), Germany.
- [30] A. Witry And M. H. Al-Hajeri And Ali A. Bondok, " Cfd Analyses Of Fluid Flow And Heat Transfer In Patternedroll-Bonded Aluminium Plate Radiators", Third International Conference on CFD in the Minerals and Process Industries, CSIRO, Melbourne, Australia, 10-12 December 2003.
- [31] <http://www.scribd.com/doc/67126715/117/Heat-Exchanger-Pressure-Drop-Analysis>(last visited at 02/05/2012).
- [32] <http://en.wikipedia.org/wiki/Cryopump>(last visited at 02/05/2012).
- [33] <http://www.iter.org/mach>(last visited at 02/05/2012).
- [34] <http://www.ipr.res.in//history.html>(last visited at 02/05/2012).
- [35] <http://www.ccfе.ac.uk/>(last visited at 02/05/2012).